AD-A042 563 DAVID W TAYLOR NAVAL SHIP RESEARCH AND DEVELOPMENT CE--ETC F/G 13/10
THEORETICAL PREDICTION OF DYNAMIC WAVE LOADS ON SMALL-WATERPLAN--ETC(U)
JUL 77 R M CURPHEY, C M LEE

UNCLASSIFIED DTNSRDC-77-0061 NL

1 OF 1
ADA042563

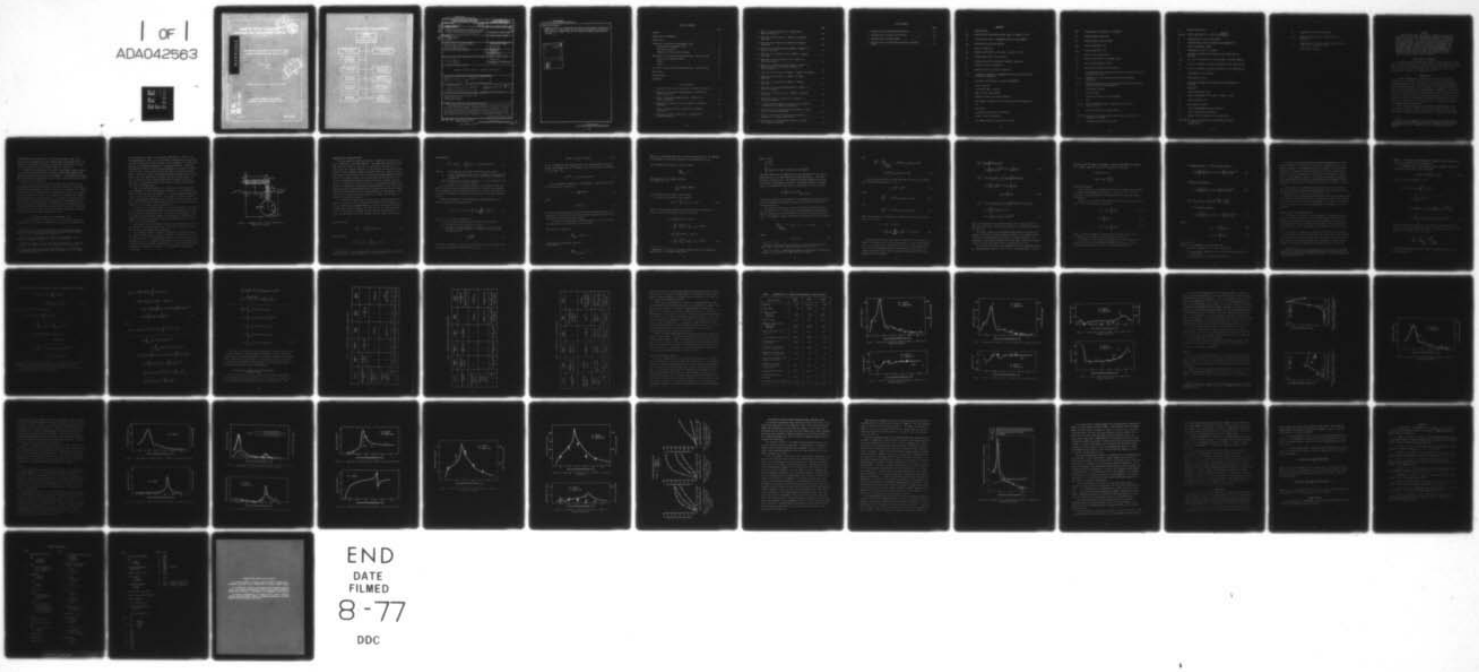

END
DATE FILMED
8-77
DDC

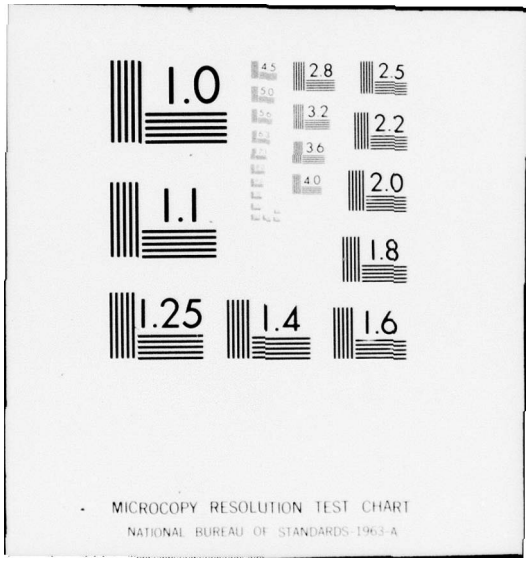
1.0
1.1
1.25
1.4
1.6
1.8
2.0
2.2
2.5
2.8
3.2
3.6
4.0
4.5
5.0
MICROCOPY RESOLUTION TEST CHART
NATIONAL BUREAU OF STANDARDS-1963-A

DAVID W. TAYLOR NAVAL SHIP
RESEARCH AND DEVELOPMENT CENTER
Bethesda, Md. 20084

THEORETICAL PREDICTION OF DYNAMIC WAVE LOADS ON SMALL-WATERPLANE-AREA, TWIN-HULL SHIPS

by

R. M. Curphey
and
C. M. Lee

SHIP PERFORMANCE DEPARTMENT
RESEARCH AND DEVELOPMENT REPORT

July 1977

Report 77-0061

Report 77-0061

THEORETICAL PREDICTION OF DYNAMIC WAVE LOADS ON SMALL-WATERPLANE-AREA, TWIN-HULL SHIPS

MAJOR DTNSRDC ORGANIZATIONAL COMPONENTS

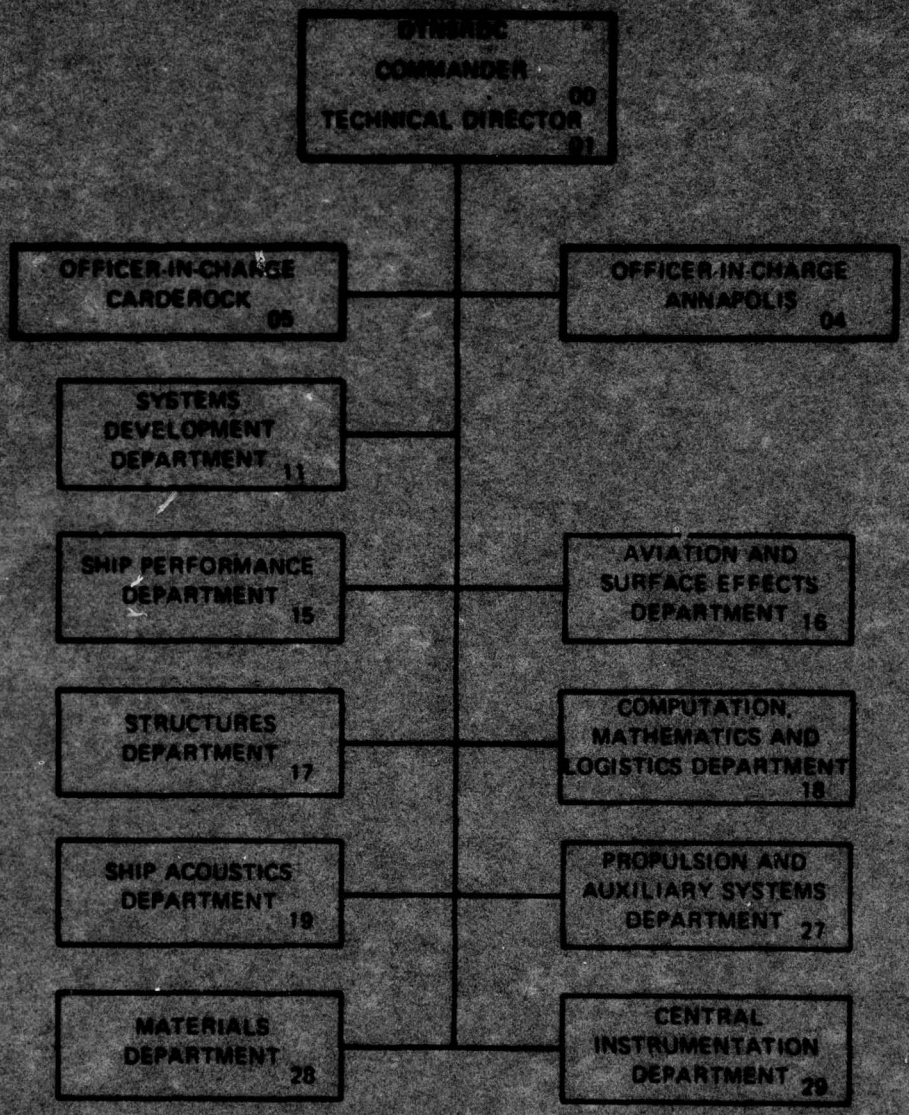

UNCLASSIFIED

SECURITY CLASSIFICATION OF THIS PAGE (When Data Entered)

REPORT DOCUMENTATION PAGE

READ INSTRUCTIONS BEFORE COMPLETING FORM

(14) 1. REPORT NUMBER: DTNSRDC-77-0061

2. GOVT ACCESSION NO.

(9) 3. RECIPIENT'S CATALOG NUMBER: Research and development rept.

(6) 4. TITLE (and Subtitle): THEORETICAL PREDICTION OF DYNAMIC WAVE LOADS ON SMALL-WATERPLANE-AREA, TWIN-HULL SHIPS

5. TYPE OF REPORT & PERIOD COVERED

6. PERFORMING ORG. REPORT NUMBER

(10) 7. AUTHOR(s): R. M. Curphey and C. M. Lee

8. CONTRACT OR GRANT NUMBER(s)

9. PERFORMING ORGANIZATION NAME AND ADDRESS: David W. Taylor Naval Ship Research and Development Center, Bethesda, Maryland 20084

10. PROGRAM ELEMENT, PROJECT, TASK AREA & WORK UNIT NUMBERS: SF43-422-001, SF43-421-202

11. CONTROLLING OFFICE NAME AND ADDRESS

(11) 12. REPORT DATE: July 1977

13. NUMBER OF PAGES: 56

14. MONITORING AGENCY NAME & ADDRESS (if different from Controlling Office)

(12) 53p.

15. SECURITY CLASS. (of this report): UNCLASSIFIED

15a. DECLASSIFICATION DOWNGRADING SCHEDULE

16. DISTRIBUTION STATEMENT (of this Report)

APPROVED FOR PUBLIC RELEASE: DISTRIBUTION UNLIMITED

17. DISTRIBUTION STATEMENT (of the abstract entered in Block 20, if different from Report)

(16) F43422, F43421

18. SUPPLEMENTARY NOTES

(17) SF43422001, SF43421202

19. KEY WORDS (Continue on reverse side if necessary and identify by block number)

Small-Waterplane-Area, Twin-Hull Ships
Dynamic Wave Loads
Ship Motion in Waves

20. ABSTRACT (Continue on reverse side if necessary and identify by block number)

A mathematical model and computer program have recently been developed to predict the bending moment, sideload, and vertical shear force acting on the cross structure and strut of twin-hull ships in beam waves. The computer program has been used to predict these loads for a variety of small-waterplane-area, twin-hull (SWATH) ships, and good agreement with experimental data confirms the basic validity of the prediction technique. The →

(Continued on reverse side)

DD FORM 1 JAN 73 1473 EDITION OF 1 NOV 65 IS OBSOLETE
S/N 0102-LF-014-6601

UNCLASSIFIED
SECURITY CLASSIFICATION OF THIS PAGE (When Data Entered)

381682

B

(Block 20 continued)

prominent feature of sideload and transverse bending-moment responses for SWATH ships is a sharp peak resulting from wave diffraction at an excitation wavelength roughly three to four times the maximum overall beam of the ship.

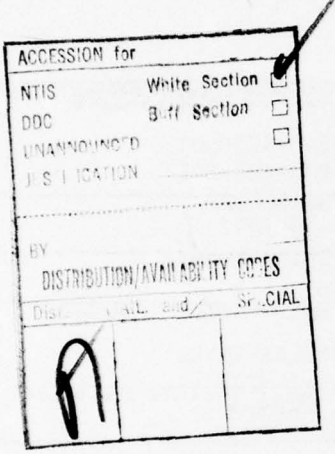

TABLE OF CONTENTS

LIST OF FIGURES

LIST OF TABLES

NOTATION

A	Wave amplitude
A_{ik}	Added inertia coefficients (i,k=2, sway; 3, heave; 4, roll)
A_p	Projected side area of submerged portion of ship demihull
A_{wp}	Waterplane area of ship demihull
a	Radius of main hull
B_{ik}	Damping coefficients (i,k=2, sway; 3, heave; 4, roll)
B_m	Maximum beam of hull cross section
b	Distance from ship centerline to demihull centerline
b_o	Breadth of strut at waterline
b_z	Breadth of strut at vertical location z
$C(z)$	Integration contour over submerged hull section from waterline to vertical coordinate z
d	Half-draft plus distance to neutral axis $\left(\frac{H}{2}+h_o\right)$
G	Green's function
g	Acceleration due to gravity
H	Draft of hull cross section
h_o	Height of neutral axis above waterline
I	Roll moment of inertia of hull cross section about origin Oyz
j	$\sqrt{-1}$
K	Wave number
L	Integration contour over left demihull
L_o	Length of ship at waterline
ℓ	Arc length about hull cross section contour

$M_3^{(o)}$	Bending moment at midpoint of crossbeam
M_2	Bending moment along strut
M_3	Bending moment along crossbeam
M_{20}	Complex amplitude of M_2
M_{30}	Complex amplitude of M_3
m	Mass of hull cross section
m_d	Mass per unit span of crossbeam section
m_h	Mass of main demihull section
m_s	Mass per unit height of strut section
$\underline{n}$	Two-dimensional unit normal vector on hull cross section contour (*positive into hull*)
n_2, n_3	Components of $\underline{n}$ in horizontal and vertical directions, respectively
Oyz	Cartesian coordinate system with origin at hull centerline and waterline (Oz-axis directed upward)
p	Hydrodynamic pressure
Q	Source strength
R	Integration contour over right demihull
t	Time
V_{is}, V_{ic}	Real and imaginary parts, respectively, of V_i, i=2,3 ($V_i = V_{ic} + j\ V_{is}$)
V_n	Normal fluid velocity on body surface
$V_2^{(o)}, V_3^{(o)}$	Transverse force and vertical shear force, respectively, at midpoint of crossbeam
V_2	Transverse shear force (side load)

V_3	Vertical shear force
V_{20}, V_{30}	Complex amplitude of V_i, i=2,3 ($V_{io}=\sqrt{V_{is}^2+V_{ic}^2}$)
Ψ	Submerged area of hull cross section
W	Two-dimensional velocity potential; see Equation (10)
x	Complex coordinate, x=y+iz
$\underline{x}$	Displacement vector in y,z plane
y,z	Cartesian coordinates with origin at hull centerline and waterline
y_o, z_o	The y and z coordinates of center of mass of portside demihull
z_B	Vertical coordinate of center of buoyancy of hull cross section
z_G	Vertical coordinate of center of gravity of hull cross section
Δ_1	Displacement of ship demihull
Δ_2	Displacement of ship
η, ζ	Cartesian coordinates with origin at hull centerline and waterline
λ	Wavelength
ξ	Complex coordinate $\xi=\eta+j\zeta$
ξ_i	Motion displacements (i=2, sway; 3, heave; 4, roll)
ξ_{io}	Complex amplitude of ξ_i
ρ	Mass density of water
Φ	Total time-dependent velocity potential
ϕ	Total complex velocity potential
ϕ_I	Complex velocity potential for incident wave
$\phi_D^{(o)}, \phi_D^{(e)}$	Odd and even component of the diffraction potential ($\phi_D=\phi_D^{(o)}+j\phi_D^{(e)}$)

ϕ_D	Complex wave diffraction potential
ϕ_c, ϕ_s	Real and imaginary parts, respectively, of ϕ ($\phi=\phi_c+j\phi_s$)
ϕ_i	Complex velocity potentials for forced oscillation (i=2, sway; 3, heave; 4, roll)
ω	Wave angular frequency

ABSTRACT

A mathematical model and computer program have recently been developed to predict the bending moment, sideload, and vertical shear force acting on the cross structure and strut of twin-hull ships in beam waves. The computer program has been used to predict these loads for a variety of small-waterplane-area, twin-hull (SWATH) ships, and good agreement with experimental data confirms the basic validity of the prediction technique. The prominent feature of sideload and transverse bending-moment responses for SWATH ships is a sharp peak resulting from wave diffraction at an excitation wavelength roughly three to four times the maximum overall beam of the ship.

ADMINISTRATIVE INFORMATION

This work has been authorized and funded by the Naval Material Command under the Small-Waterplane-Area, Twin-Hull Program, Task Funding SF43-422-001, and by the Naval Sea Systems Command under the High-Performance-Vehicle, Hydromechanics Program, Task Funding SF43-421-202.

INTRODUCTION

A primary consideration in the design of twin-hull ships is the strength of the crossbeam structure and struts necessary to sustain the wave-induced dynamic loads. One phase of the ongoing research program of the small-waterplane-area, twin-hull (SWATH) ship concept at the David W. Taylor Naval Ship Research and Development Center (DTNSRDC) is the development of an analytical method to predict dynamic loading on twin-hull ships in waves. A mathematical model and computer-prediction tool are now available which provide the transverse bending moment, sideload, and vertical shear force acting on the crossbeam and struts of twin-hull ships, having zero forward speed, in beam waves.[1]

From a structural viewpoint, the transverse bending moment on the crossbeam and struts is the most critical of the loads, and arises from the action of both wave forces and ship motion. Furthermore, experiments

---

[1] Curphey, R. M., "Computation of Loads Acting on the Cross Structure and Struts of Twin Hull Ships in Beam Waves," DTNSRDC Departmental Report SPD-651-01 (Nov 1975). A complete listing of references is given on page 43.

on SWATH models[2] have shown that the most severe dynamic loads on the cross deck are experienced at zero forward speed in beam waves; hence, the theoretical formulation is limited to predicting loads acting in a transverse ship section for the zero-speed, beam-wave condition.

The prediction technique has been used to investigate dynamic loading for a variety of twin-hull ships, including conventional catamarans and SWATH ships with one and two struts per demihull. The generally good agreement with available experimental results tends to confirm the basic validity of the theoretical formulation.

In the first section of this report theoretical formulation of the load-prediction method is described. Some basic elements of the loading theory have been presented in previous reports by the authors.[3,4,5] However, this section of the report provides a comprehensive and up-to-date description of the theoretical basis for the twin-hull, load-prediction computer program currently in use at the Center.[1] In subsequent sections of the report, computed transverse loads are presented for several SWATH ships in regular and irregular beam waves, and comparisons with available results of model experiments are made. The prominent features and trends of the load responses are discussed, and important distinctions between the loading on SWATH ships and conventional catamarans are noted.

THEORETICAL PREDICTION OF HYDRODYNAMIC LOADS

A theoretical analysis is described in this section for determining dynamic loads on the hull of a SWATH ship. The analysis is limited to the

---

[2]Jones, H. D. and D. M. Gerzina, "Motions and Hull-Induced Bridging Structure Loads for a Small Waterplane Area, Twin-Hulled Attack Aircraft Carrier in Waves," NSRDC Report 3819 (Aug 1973).

[3]Lee, C. M. et al., "Prediction of Motion and Hydrodynamic Loads of Catamarans," Marine Technology, Vol. 10, No. 4 (Oct 1973).

[4]Curphey, R. M. and C. M. Lee, "Analytical Determination of Structural Loading on ASR Catamaran in Beam Seas," NSRDC Report 4267 (Apr 1974).

[5]Pien, P. C. and C. M. Lee, "Motion and Resistance of Low-Waterplane Area Catamarans," Ninth Symposium on Naval Hydrodynamics, Vol. 1, Office of Naval Research (1972).

loads acting in the plane of a transverse cross section. That is, only the bending moments, shear forces, and tensile (compressive) forces on the cross deck and struts as shown in Figure 1 are considered. To simplify the analysis, the following assumptions or conditions are made. The fluid surrounding the body is inviscid and incompressible; its motion is irrotational so that a velocity potential function $\Phi(\underline{x},t)$ exists in the fluid domain. The body is subject to regular beam waves, responds freely to the waves in the sway, heave, and roll modes, and has no forward speed. The ship is replaced by twin cylinders, which have a uniform cross section identical to the midship section of the ship and a length that maintains the actual ship displacement.

Under the foregoing assumptions or conditions, the loading analysis can be reduced to a cross section plane; see Figure 1. For a SWATH ship, there are three main structural members, i.e., the submerged main hull, the vertical struts, and the cross deck. The loadings of practical interest are the bending moments and shear forces induced on the strut and the cross deck, especially at both the middle and the junctures of the main structural members, i.e., cross deck, strut, and main hull.

The analysis is first developed for loads at the midpoint of the cross deck or beam; then the midpoint loads are used to evaluate loads at other points along the crossbeam and strut. This method is advantageous in that the midpoint-load formulation exhibits certain simplicity resulting from symmetry of the ship section and inertial and hydrodynamic forces with respect to the section centerline.

Expressions for the wave loads contain the wave-induced motion; hence, the equations of motion for heave, sway, and roll are solved as an intermediate step in the midpoint-load computation.

The coordinate system to be used in the analysis is shown in Figure 1. The location of the center of gravity of the body is indicated by z_G, and the center of gravity of the right-half portion of the cross section is indicated by (y_o,z_o). The height of the neutral axis of the cross deck above the mean surface of the water is denoted by h_o. A plane, progressive sinusoidal wave of amplitude A and length λ is propagating in the positive y direction.

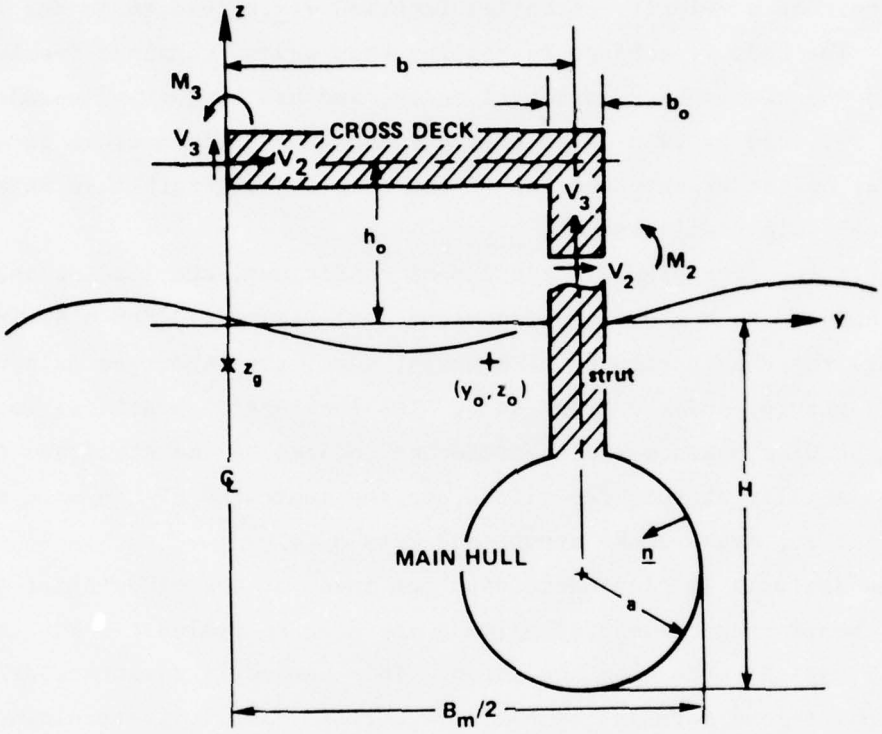

Figure 1 - Schematic View of Type of Loading on a SWATH Cross Section

FORMULATION OF CENTERLINE LOADS

From principles of rigid body mechanics, stresses on the ship section may be obtained by a free-beam approach. This means that a portion of the body (the ship section in this case) is isolated by "cutting" it at the points where the loads are desired, and the stresses are then given by summing all forces or moments acting on one side of the cut. Since the absolute value of a given load at the cut should be the same regardless of which portion of the body is taken to be the free end, the load may also be obtained by averaging with appropriate sign the forces or moments from the parts of the body on both sides of the cut. This approach was suggested by Ogilvie for evaluation of longitudinal bending moments on ships,[6] and it has been applied here to determining loads in a transverse ship section. When loads are to be evaluated at the crossbeam midpoint by evaluating the forces over the entire section, use can be made of the symmetry of the ship to simplify the loading expressions.

Let m denote the mass of the cross section; p, the hydrodynamic pressure; $\underline{n} = (n_2, n_3)$, the unit normal vector pointing into the body; ξ_2, ξ_3, and ξ_4, respectively, the displacement of the body from its mean position in sway, heave, and roll; $\int_{R+L} d\ell$, the integral over the submerged contour of the cross section on the right and left sides at the mean position. Then, the expressions for various loadings per unit length can be written as

Horizontal Shear

$$V_2^{(o)} = -\frac{1}{2} \int_{R+L} pn_2 \, \mathrm{sgn}(y) \, d\ell \tag{1}$$

Vertical Shear

$$V_3^{(o)} = \frac{1}{2} m y_o \ddot{\xi}_4 - \frac{1}{2} \int_{R+L} pn_3 \, \mathrm{sgn}(y) \, d\ell \tag{2}$$

---

[6] Ogilvie, T. F., "On the Computation of Wave-Induced Bending and Torsion Moment," Journal of Ship Research, Vol. 15, No. 3 (1971).

Bending Moment

$$M_3^{(o)} = \frac{1}{2} m y_o \ddot{\xi}_3 - \frac{1}{2} \int_{R+L} p[n_3|y| + n_2(h_o - z)\mathrm{sgn}(y)]d\ell \qquad (3)$$

where m is the mass per unit length of the hull cross section

y_o is the y-coordinate of the center of gravity of the right-half portion of the hull cross section, the double dot denotes the acceleration

sgn(y) means the sign of the y variable, i.e., on the right-half side $y>0$ and on the left-half side $y<0$.

As can be seen in the foregoing formulas, to evaluate the loads, the motion of the body and the pressure distribution on the hull are required. This information can be obtained by solving for a velocity potential function, which represents the disturbed flow field due to both waves and body motion.

Under the assumption of an infinitesimally small disturbance, the velocity potential can be expressed by

$$\Phi(y,z,t) = \phi(y,z)e^{-j\omega t} = \left(\phi_I + \phi_D + \sum_{i=2}^{4} \phi_i \xi_{io}\right) e^{-j\omega t} \qquad (4)$$

where ξ_{io} is the complex amplitude of ξ_i

ϕ_I is the complex potential which represents incoming waves

ϕ_D represents the wave-diffraction potential

ϕ_i represents the fluid disturbance caused by body motion in the ith mode. The wave frequency ω is related to the wave length λ in deep water by

$$\omega = \sqrt{\frac{2\pi g}{\lambda}} \qquad (5)$$

and $j=\sqrt{-1}$. In Equation (4) the velocity potentials on the right-hand side are given in the form of complex potential, e.g.,

$$\phi(y,z) = \phi_c(y,z) + j\phi_s(y,z) \tag{6}$$

and it is understood that when the product of a complex spatial function and the time harmonic term $e^{-j\omega t}$ appears, only the real part of the product is to be taken, i.e.,

$$\phi e^{-j\omega t} = \phi_c \cos \omega t + \phi_s \sin \omega t \tag{7}$$

The incoming-wave potential ϕ_I, corresponding to surface waves of the form A cos (Ky-ωt), is given by

$$\phi_I = - \frac{jgA}{\omega} e^{Kz+jKy} \tag{8}$$

where

$$K = \frac{2\pi}{\lambda} = \frac{\omega^2}{g} \tag{9}$$

The diffracted-wave potential ϕ_D and the motion-generated potentials ϕ_i are determined by the method of source distribution from known values of the normal fluid velocity on the hull surface.

If a harmonic function W(y,z) represents either ϕ_i or ϕ_D, the boundary conditions to be satisfied by W are as follows.

The Free-Surface Condition

$$\left.\frac{\partial W}{\partial z}\right|_{z=0} - KW(y,0) = 0$$

The Kinematic Body-Boundary Condition
(Solid Surface)

$$\left.\frac{\partial W}{\partial n}\right|_{\text{Body Surface}} = V_n$$

where V_n is the normal velocity of the body surface for ϕ_1 or the negative of the normal fluid velocity induced by the incoming wave for ϕ_D.

The Vanishing Fluid Velocity at Infinite Depth

$$\left.\frac{\partial W}{\partial z}\right|_{z=-\infty} = 0$$

The Requirement for Outgoing, Radiated, Plane Waves at $|y|=\infty$

$$\lim_{y \to \mp\infty} \operatorname{Re}\left(\frac{\partial W}{\partial y} \mp jKW\right) = 0$$

where Re means the real part of what follows.

The potential function W can be given by

$$W(y,z) = \int_R Q(\eta,\zeta) G(y,z;\eta,\zeta) d\ell \tag{10}$$

where Q is the unknown strength of the sources, and the expression of source G given by Wehausen and Laitone[7] (p. 481) is

$$\begin{aligned} G = \frac{1}{2\pi} \operatorname{Re}_j \Bigg[& \log(x-\xi) - \log(x-\bar{\xi}) \\ & + 2 \int_0^\infty \frac{e^{-jK(x-\bar{\xi})}}{K-k} dk \Bigg] - j \operatorname{Re}_j e^{-jK(x-\bar{\xi})} \\ \mp \frac{1}{2\pi} \operatorname{Re}_j \Bigg[& \log(x+\bar{\xi}) - \log(x+\xi) \\ & + 2 \int_0^\infty \frac{e^{-jK(x+\xi)}}{K-k} dk \Bigg] \mp j \operatorname{Re}_j e^{-jK(x+\xi)} \end{aligned} \tag{11}$$

---

[7] Wehausen, J. V. and E. V. Laitone, "Surface Waves," Encyclopedia of Physics, Vol. IX, Springer Verlag, 1960.

where $x = y+jz$

$\xi = \eta+j\zeta$

$\bar{\xi} = \eta-j\zeta$

$\int_0^\infty$ denotes the Cauchy principal value integral.

The upper signs are to be taken when W is an even function of y, and the lower signs are to be taken when W is an odd function of y. The Green function G satisfies all of the boundary conditions imposed on W, except the kinematic body-boundary condition. The unknown function Q is determined by satisfying the normal velocity conditions on the hull boundary,

$$\frac{\partial}{\partial n}\int_R QGd\ell = V_n(y,z)\Big|_{\text{Body Surface}}$$

The previous equation can be reduced to a Freidholm-type integral equation for Q, and details of procedures for numerical solution are described in References 8 and 9.

The velocity potential ϕ_3, which is associated with heave motion, is an even function of y; ϕ_2 and ϕ_4, which are associated with sway and roll motion, respectively, are odd functions; ϕ_D has both even and odd components. The kinematic boundary conditions to be satisfied by these potentials are

$$\left.\frac{\partial\phi_i}{\partial n}\right|_{\substack{\text{Body}\\\text{Surface}}} = -j\omega n_i \quad \text{for} \quad i = 2, 3, \text{ and } 4 \tag{12}$$

where

$$n_4 = yn_3 - zn_2 \tag{13}$$

---

[8] Frank, W., "Oscillation of Cylinders in or Below the Free Surface of Deep Fluids," David Taylor Model Basin Report 2375 (Oct 1967).

[9] Lee, C. M. et al., "Added Mass and Damping Coefficients of Heaving Twin Cylinders in a Free Surface," NSRDC Report 3695 (1971).

and

$$\frac{\partial \phi_D}{\partial n} = - \frac{\partial \phi_I}{\partial n}\bigg|_{\substack{\text{Body} \\ \text{Surface}}} = - \omega A e^{Kz}(n_2 \cos Ky + n_3 \sin Ky)$$

$$+ j\omega A e^{Kz}(n_2 \sin Ky - n_3 \cos Ky) \tag{14}$$

The diffraction potential can be expressed as the sum of an odd and even component with respect to y, i.e.,

$$\phi_D = \phi_D^{(o)} + j\phi_D^{(e)} \tag{15}$$

where

$$\frac{\partial \phi_D^{(o)}}{\partial n} = - \omega A e^{Kz}(n_2 \cos Ky + n_3 \sin Ky) \tag{16}$$

and

$$\frac{\partial \phi^{(e)}}{\partial n} = - \omega A e^{Kz}(n_3 \cos Ky - n_2 \sin Ky) \tag{17}$$

When the potentials are evaluated, the pressure at any point on the hull surface is given by

$$p = - \rho \phi_t - \rho g(\xi_3 + y\xi_4)$$

$$= j\omega\rho \left(\phi_I + \phi_D + \sum_{i=2}^{4} \phi_i \xi_{io}\right) e^{-j\omega t} - \rho g(\xi_3 + y\xi_4) \tag{18}$$

Substitution of the pressure given by Equation (18) into Equations (1) through (3) and use of the even and odd properties of the potential functions ϕ_I, ϕ_D, and ϕ_i and n_2 and n_3 with respect to the ship centerline results in the following expressions for the transverse force $V_2^{(o)}$, the vertical shear force $V_3^{(o)}$, and the transverse bending moment $M_3^{(o)}$ at the midpoint of the cross beam.

$$V_2^{(o)} = \left[-\rho g A \int_R e^{Kz} \cos Ky \; n_2 d\ell \right.$$

$$\left. -j\rho\omega \int_R \phi_D^{(e)} n_2 d\ell \right] e^{-j\omega t} - j\omega\rho \; \xi_3 \int_R \phi_3 n_2 d\ell \qquad (19)$$

$$V_3^{(o)} = -\frac{\omega^2}{2} m y_o \xi_4 + \rho g b b_o \xi_4 + \left[-j\rho g A \int_R e^{Kz} \sin Ky \; n_3 d\ell \right.$$

$$\left. -j\omega\rho \int_R \phi_D^{(o)} n_3 d\ell \right] e^{-j\omega t} - j\omega\rho\xi_2 \int_R \phi_2 n_3 d\ell$$

$$-j\omega\rho\xi_4 \int_R \phi_4 n_3 d\ell \qquad (20)$$

$$M_3^{(o)} = -\frac{\omega^2}{2} m y_o \xi_3 + \rho g b b_o \xi_3 + \left[-\rho g A \int_R e^{Kz} \cos Ky \{n_3 y + (h_o - z) n_2\} d\ell \right.$$

$$-j\omega\rho \int_R \phi_D^{(e)} \{n_3 y + n_2 (h_o - z)\} d\ell$$

$$\left. -j\omega\rho\xi_3 \int_R \phi_3 \{n_3 y + n_2 (h_o - z)\} d\ell \right] e^{-j\omega t} \qquad (21)$$

where the expression for ϕ_I given by Equation (8) is used, and $\phi_D^{(e)}$ and $\phi_D^{(o)}$ mean, respectively, the even and odd part of ϕ_D, defined by Equations (16) and (17).

The dynamic loads at the crossbeam midpoint given by Equations (19) through (21) exhibit a certain simplicity because of the symmetry properties of the forces involved with respect to the ship centerline. In particular, it is noted that heave is the only mode of motion contributing to $M_3^{(o)}$ and $V_2^{(o)}$, while sway and roll contribute only to $V_3^{(o)}$.

If we remove the harmonic time dependence from the foregoing equations, the remaining expressions are in the form of complex amplitude. The real

amplitudes and the phases with respect to the incoming waves are obtained for a complex amplitude V_o, which is expressed by $V_o = V_c + jV_s$

$$\text{Amplitude} = |V_o|$$

$$\text{Phase} = \tan^{-1}\left(\frac{-V_s}{V_c}\right)$$

EQUATIONS OF MOTION

The expressions for the midpoint loads given in Equations (19) through (21) contain the amplitudes of motion ξ_2, ξ_3, and ξ_4. It is therefore necessary to solve the equations of motion before the loads can actually be evaluated.

Relative to the origin of the coordinate system Oyz, the equations for sway, heave, and roll motion are given by

$$m\ddot{\xi}_2 - mz_G\ddot{\xi}_4 = \int_{R+L} pn_2 d\ell \tag{22}$$

$$m\ddot{\xi}_3 = \int_{R+L} pn_3 d\ell \tag{23}$$

$$I\ddot{\xi}_4 - mz_G\ddot{\xi}_2 = \int_{R+L} pn_4 d\ell \tag{24}$$

where I is the roll moment of inertia about the origin, and z_G is the z-coordinate of the center of gravity of the cross section.

Substitution of the pressure from Equation (18) into Equations (22) through (24) and use of the symmetry properties of ϕ_I, ϕ_D, ϕ_i, and n_i about the ship centerline result in the following expressions.

$$\{-\omega^2(m+A_{22})-j\omega B_{22}\}\xi_2 + \{-\omega^2 m(-z_G)-\omega^2 A_{24}-j\omega B_{24}\}\xi_4$$

$$= 2\rho\omega A\left[\frac{jg}{\omega}\int_R e^{Kz}n_2 \sin Kyd\ell + j\int_R \phi_D^{(o)}n_2 d\ell\right]e^{-j\omega t} \tag{25}$$

$$\{-\omega^2(m+A_{33})-j\omega B_{33}+2\rho g b_o\}\xi_3$$

$$= 2\rho\omega A\left[\frac{g}{\omega}\int_R e^{Kz}n_3 \cos Kyd\ell - \int_R \phi_D^{(e)}n_3 d\ell)\right]e^{-j\omega t} \tag{26}$$

$$\left\{-\omega^2(I+A_{44})-j\omega B_{44} + \rho g\left[2b_o\left(b+\frac{b_o^3}{12}\right) - \forall z_B\right]\right\}\xi_4$$

$$+\{-\omega^2(-mz_G+A_{42})-j\omega B_{42}\}\xi_2$$

$$= 2\rho\omega A\left[\frac{jg}{\omega}\int_R e^{Kz}n_4 \sin Kyd\ell + j\int_R \phi_D^{(o)}n_4 d\ell\right]e^{-j\omega t} \tag{27}$$

where

$$A_{ik} = -\frac{2\rho}{\omega}\int_R \phi_{is}n_k d\ell \tag{28}$$

$$B_{ik} = 2\rho\int_R \phi_{ic}n_k d\ell \tag{29}$$

for i, k=2, 3, 4.

where $\forall$ is the immersed cross sectional area,

z_B is the z-coordinate of the center of buoyancy,

b is the distance between the ship centerline and the centerline of one hull, and

b_o is the breadth of the strut at the waterline.

The terms involving the diffraction potential appearing on the right side of Equations (25) through (27) are usually evaluated by use of the Haskind relation. By the Haskind method, the integrals of the diffraction potential are replaced by integrals involving the forced oscillation potentials so that the diffraction potential need not be explicitly determined. In this analysis, however, the diffraction potential is needed for load computation* and is explicitly computed by using the method of source distribution taken from the hull-boundary conditions of Equations (16) and (17).

The equivalence of evaluating wave-exciting forces by the Haskind method and by direct computation and integration of the diffraction potential has been verified during the course of this work.

When all of the required potential functions and resulting wave-exciting forces and hydrodynamic coefficients are evaluated, Equations (25) through (27) can be solved for the motion displacements ξ_2, ξ_3, and ξ_4. With known motion, the equations for the loads (Equations (19) through (21)) can be evaluated.

FORMULATION OF OFF-CENTERLINE LOADS

The dynamic loads (shear, tension/compression, and bending moment) at points other than the midpoint of the crossbeam can be obtained by either adding to or subtracting from the loads at the midspan of the cross deck the appropriate effects contributed by the segment of the structural members between the section in question and the midspan section of the cross deck.

For the sake of simplicity, we assume that the mass per unit length is uniform along the cross deck and along the vertical strut cross sections and is denoted by m_d and m_s, respectively. We denote the mass of the main hull section on the right side by m_h, and the main hull center of mass is assumed to be along the centerline of the main hull cross section; see

*Ogilvie[6] has shown that the diffraction contribution to the bending moment may be obtained by a Haskind-type relation. This method still involves the solution of two new potential functions so no real computational advantages are provided.

Figure 1. The loads to be determined are limited to those acting in sections of the strut and the cross deck only.

The expression for the horizontal force at a location y along the cross beam $V_2(y,h_o)$ can be easily obtained by

$$V_2(y,h_o) = V_2^{(o)}+\omega^2 m_d y(\xi_2-h_o\xi_4) \tag{30}$$

and at a location z along the strut by

$$V_2(b,z) = V_2(b,h_o)-m_s\int_z^{h_o}(\ddot{\xi}_2-z\ddot{\xi}_4)dz$$

$$+j\omega\rho\int_{C(z)}\phi n_2 d\ell e^{-j\omega t}$$

$$= V_2^{(o)}+\omega^2\left\{m_d b+m_s(h_o-z)\right\}\xi_2-\omega^2\left\{m_d b h_o+m_s\frac{(h_o^2-z^2)}{2}\right\}\xi_4$$

$$+j\omega\rho\int_{C(z)}(\phi_I+\phi_D+\phi_2\xi_{20}+\phi_3\xi_{30}+\phi_4\xi_{40})n_2 d\ell e^{-j\omega t} \tag{31}$$

where the integral C(z) denotes the line integral along the left side of one strut from the waterline to the point in consideration and back to the waterline on the right side of the strut, i.e.,

$$\int_{C(z)} = \int_0^z\Big|_{\substack{\text{Left}\\\text{Side}}} + \int_z^0\Big|_{\substack{\text{Right}\\\text{Side}}}$$

and the terms below the dashed line should be added only when $z<0$, i.e., below the waterline.

The vertical force at a location y along the crossbeam can be obtained by

$$V_3(y,h_o) = V_3^{(o)} - m_d \int_0^y (\ddot{\xi}_3 + y\ddot{\xi}_4)dy$$

$$= V_3^{(o)} + \omega^2 m_d y\xi_3 + \omega^2 m_d \frac{y^2}{2} \xi_4 \qquad (32)$$

and at a location z along the strut by

$$V_3(b,z) = V_3(b,h_o) - m_s \int_z^{h_o} (\ddot{\xi}_3 + b\ddot{\xi}_4)dz$$

$$- -$$

$$+ j\omega\rho \int_{C(z)} \phi n_3 d\ell e^{-j\omega t} - \rho g \int_{C(z)} (\xi_3 + y\xi_4) n_3 d\ell$$

$$= V_3^{(o)} + \omega^2 m_d b\xi_3 + \omega^2 m_d \frac{b}{2} \xi_4 + \omega^2 m_s (h_o - z)\xi_3$$

$$+ \omega^2 m_s b(h_o - z)\xi_4$$

$$- -$$

$$+ j\omega\rho \int_{C(z)} (\phi_I + \phi_D + \phi_2\xi_{20} + \phi_3\xi_{30} + \phi_4\xi_{40}) n_3 d\ell e^{-j\omega t}$$

$$- \rho g(b_o - b_z)\xi_3 - \rho g(b_o - b_z)b\xi_4 \qquad (33)$$

where b_z is the breadth of the strut at z. If the strut is vertical, the contribution from the components below the dashed line will be zero.

The bending moments at points along the crossbeam and strut denoted by M_3 and M_2, respectively, can be obtained by

$$M_3(y,h_o) = M_3^{(o)} - yV_3^{(o)} + m_d \int_0^y (y-\eta)(\ddot{\xi}_3 + \eta\ddot{\xi}_4)d\eta$$

$$= M_3^{(o)} - \omega^2 m_d \frac{y^2}{2} \xi_3 - \omega^2 m_d \frac{y^3}{6} \xi_4 - \omega^2 m y_o \frac{y}{2} \xi_4$$

$$-\rho g y b b_o \xi_4 + \left[j\rho g y A \int_R e^{Kz} n_3 \sin Ky d\ell + j\rho\omega y \int_R \phi_D^{(o)} n_3 d\ell \right] e^{-j\omega t}$$

$$+ j\rho\omega y \xi_2 \int_R \phi_2 n_3 d\ell + j\omega\rho y \xi_4 \int_R \phi_4 n_3 d\ell \qquad (34)$$

and

$$M_2(b,z) = M_3(b,h_o) - (h_o - z)V_2(b,h_o) - m_s \int_z^{h_o} (z-\zeta)(\ddot{\xi}_2 - \zeta\ddot{\xi}_4)d\zeta$$

$$+ i\omega\rho \int_{C(z)} \phi\{(\eta-b)n_3 - (\zeta-z)n_2\} d\ell e^{-j\omega t}$$

$$-\rho g \int_{C(z)} (\xi_3 + b\xi_4)\{(\eta-b)n_3 - (\zeta-z)n_2\} d\ell$$

$$= M_3^{(o)} + \left[j\rho g b A \int_R e^{Kz} n_3 \sin Ky d\ell + \rho g (h_o - z) A \int_R e^{Kz} n_2 \sin Ky d\ell \right.$$

$$\left. + j\rho\omega b \int_R \phi_D^{(o)} n_3 d\ell + j\rho\omega (h_o - z) \int_R \phi_D^{(e)} n_2 d\ell \right] e^{-j\omega t}$$

$$+ \left[-\omega^2 m_d b (h_o - z) - \omega^2 m_s \frac{(h_o - z)^2}{2} + j\rho\omega b \int_R \phi_2 n_3 d\ell \right] \xi_2$$

$$+ \left[-\omega^2 m_d \frac{b^2}{2} + j\rho\omega (h_o - z) \int_R \phi_3 n_3 d\ell \right] \xi_3$$

$$+\left[-\omega^2 m_d \frac{b^3}{6} + \frac{\omega^2}{2} y_o bm + \omega^2 m_d b h_o (h_o - z) - \rho g b_o b^2 \right.$$

$$\left. + \omega^2 m_s \frac{(2h_o^3 + z^3 - 3zh_o^2)}{6} + j\rho\omega b \int_R \phi_4 n_3 d\ell \right] \xi_4$$

$$+\left[j\rho\omega \int_{C(z)} \phi_I \{(\eta - b)n_3 - (\zeta - z)n_2\} d\ell \right.$$

$$\left. + j\rho\omega \int_{C(z)} \phi_D \{(\eta - b)n_3 - (\zeta - z)n_2\} d\ell \right] e^{-j\omega t}$$

$$+ j\rho\omega \int_{C(z)} \phi_2 \{(\eta - b)n_3 - (\zeta - z)n_2\} d\ell \xi_2$$

$$+ j\rho\omega \int_{C(z)} \phi_3 \{(\eta - b)n_3 - (\zeta - z)n_2\} d\ell \xi_3$$

$$+ j\rho\omega \int_{C(z)} \phi_4 \{(\eta - b)n_3 - (\zeta - z)n_2\} d\ell \xi_4 \qquad (35)$$

The loads at different locations, decomposed to show the contributions of various sources, are shown in Tables 1 through 3. A zero subscript is used to denote the complex amplitudes. The loads obtained in the foregoing are the quantities per unit length of the ship; thus, the total loads on the ship can be approximated by multiplying the sectional quantities by the equivalent ship length as previously mentioned.

PREDICTION OF LOADS ON SMALL-WATERPLANE-AREA, TWIN-HULL SHIPS

Over the past several years, the theoretical load-prediction model described previously has been applied to both conventional catamarans and newly designed small-waterplane-area, twin-hull (SWATH) models. Load

TABLE 1 - DECOMPOSITION OF HORIZONTAL SHEAR FORCES

Location	Incoming Wave	Diffracted Wave	Sway Motion	Heave Motion	Roll Motion
Cross Deck Midpoint $V_{20}(0,h_o)$	$-\rho g A \int_R (n_2 e^{Kz} \cos Ky)d\ell$	$-j\rho\omega \int_R \phi_D^{(e)} n_2 d\ell$	0	$-j\omega\rho \int_R \phi_3 n_3 d\ell$	0
Along Cross Deck $V_{20}(y,h_o)$ $= V_{20}(0,h_o)$ + =>	0	0	$+\omega^2 m_d y \xi_{20}$	0	$-\omega^2 m_d h_o y \xi_{40}$
Along Strut $(z<h_o)$ $V_{20}(b,z)$ $= V_{20}(b,h_o)$ + =>	0	0	$-\omega^2 m_s (h_o - z)\xi_{20}$	0	$+m_s \left(\frac{h_o^2 - z^2}{2}\right) \xi_{40}$
+ => Add if $z<0$	$+j\omega\rho \int_{C(z)} \phi_I n_2 d\ell$	$+j\omega\rho \int_{C(z)} \phi_D n_2 d\ell$	$+j\omega\rho\xi_{20} \int_{C(z)} \phi_2 n_2 d\ell$	$+j\omega\rho\xi_{30} \int_{C(z)} \phi_3 n_2 d\ell$	$+j\omega\rho\xi_{40} \int_{C(z)} \phi_4 n_2 d\ell$

TABLE 2 - DECOMPOSITION OF VERTICAL SHEAR FORCES

Location	Incoming Wave	Diffracted Wave	Sway Motion	Heave Motion	Roll Motion
Cross Deck Midpoint $V_{30}(0,h_o)$	$-\rho gA\int_R (n_3 e^{Kz} \sin Ky)d\ell$	$-j\omega\rho\int_R \phi_D^{(o)} n_3 d\ell$	$-j\omega\rho\xi_{20}\int_R \phi_2 n_3 d\ell$	0	$-j\omega\rho\xi_{40}\int_R \phi_4 n_3 d\ell + \left(\rho g b b_o - \frac{\omega^2}{2} m y_o\right)\xi_{40}$
Along Cross Deck $V_{30}(y,h_o) = V_{30}(0,h_o) + \Rightarrow$	0	0	0	$+\omega^2 m_d y \xi_{30}$	$+\omega^2 m_d \frac{y^2}{2}\xi_{40}$
Along Strut $(z<h_o)$ $V_{30}(b,z) = V_{30}(b,h_o) + \Rightarrow$	0	0	0	$+\omega^2 m_s (h_o - z)\xi_{30}$	$+\omega^2 m_s b(h_o - z)\xi_{40}$
$+ \Rightarrow$ Add if $z<0$	$+j\omega\rho\int_{C(z)} \phi_I n_3 d\ell$	$+j\omega\rho\int_{C(z)} \phi_D n_3 d\ell$	$+j\omega\rho\xi_{20}\int_{C(z)} \phi_2 n_3 d\ell$	$+j\omega\rho\xi_{30}\int_{C(z)} \phi_3 n_3 d\ell - \rho g(b_o - b_z)\xi_{30}$	$+j\omega\rho\xi_{40}\int_{C(z)} \phi_4 n_3 d\ell - \rho g b(b_o - b_z)\xi_{40}$

TABLE 3 - DECOMPOSITION OF BENDING MOMENT

Location	Incoming Wave	Diffracted Wave	Sway Motion	Heave Motion	Roll Motion
Cross Deck Midpoint $M_{30}(0,h_o)$	$-\rho gA\int_R [e^{Kz}\cos Ky \{n_3 y+(h_o-z)n_2\}]d\ell$	$-j\rho\omega\int_R \phi_D^{(e)}\{n_3 y +(h_o-z)n_2\}d\ell$	0	$-\frac{\omega^2}{2} m y_o \xi_{30}+\rho g b b_o \xi_{30}$ $-j\rho\omega\xi_{30}\int_R \phi_3\{n_3 y +(h_o-z)n_2\}d\ell$	0
Along Cross Deck $M_{30}(y,h_o)$ = $M_{30}(0,h_o)$ + -->	$+j\rho gyA\int_R e^{Kz}n_3$ sin $Kyd\ell$	$+j\rho\omega y\int_R \phi_D^{(o)}n_3 d\ell$	$+j\rho\omega y\xi_{20}\int_R \phi_2 n_3 d\ell$	$-\omega^2 m_d \frac{y^2}{2}\xi_3$	$\frac{\omega^2}{2} m y y_o \xi_{40}$ $-\rho g y b b_o \xi_{40}-\omega^2 m_d \frac{y^3}{6}\xi_{40}$ $+j\rho\omega y\xi_{40}\int_R \phi_4 n_3 d\ell$
Along Strut ($z<h_o$) $M_2(b,z)$ = $M_{30}(b,h_o)$ + -->	$(h_o-z)\rho gA\int_R e^{Kz}n_2 \cos Kyd\ell$	$(h_o-z)j\rho\omega\int_R \phi_D^{(e)}n_2 d\ell$	$-\omega^2 m_d b(h_o-z)\xi_{20}$ $-\omega^2 m_s \frac{(h_o-z)^2}{2}\xi_{20}$	$+j\rho\omega(h_o-z)\xi_{30}\int_R \phi_3 n_3 d\ell$	$+\omega^2 m_d b h_o(h_o-z)\xi_{40}$ $+\frac{\omega^2 m_s}{6}(2h_o^3+z^3-3zh_o^2)$
+ --> Add if $z<0$	$+j\rho\omega\int_{C(z)} \phi_I\{(\eta-b)n_3 -(\zeta-z)n_2\}d\ell$	$+j\omega\rho\int_{C(z)} \phi_D\{(\eta-b)n_3 -(\zeta-z)n_2\}d\ell$	$+j\rho\omega\int_{C(z)} \phi_2\{(\eta-b)n_3 -(\zeta-z)n_2\}d\ell\xi_{20}$	$+j\rho\omega\int_{C(z)} \phi_3\{(\eta-b)n_3 -(\zeta-z)n_2\}d\ell\xi_{30}$	$+j\rho\omega\int_{C(z)} \phi_4\{(\eta-b)n_3 -(\zeta-z)n_2\}d\ell\xi_{40}$

prediction results for conventional catamarans have been reported in References 3 and 4. The overall good agreement of the prediction with experimentally obtained loads has confirmed the basic validity of the theory for the conventional catamaran hull forms.

In this report load prediction results for several SWATH hull forms are presented and compared with available load measurements on models, and the essential features of transverse loading responses on SWATH type vehicles are discussed. The results presented here are for single-strut SWATH designs, since these hull forms are compatible with the two-dimensional approximations of the theory and adequate experimental data for these ships is now available for comparison. Application of the theory to the prediction of loads on double strut, i.e., struts in tandem, SWATH forms, and stable platforms has been accomplished with some limited success by a strip-wise approach; however, very little experimental data are available to validate predictions for these types of hulls.

Models of several SWATH ship designs have been built and tested at the Center in recent years. In particular wave-induced motions and loads have been measured on SWATH 1, SWATH 4, and SWATH CVA (attack aircraft carrier) models, and the results of these model experiments have naturally been the subject of extensive analysis and comparison with the theoretical load and motion predictions. A compilation of full-scale geometric characteristics of the previously described models is shown in Table 4.

SWATH ATTACK AIRCRAFT CARRIER

The most comprehensive set of experimental loading data for a SWATH ship was obtained for a proposed SWATH CVA; see Reference 2. The amplitude and phase of the wave-induced loads acting on the ship crossbeam together with the ship motions were measured over a range of speeds and wave headings. The theoretical load prediction (Equations (19) through (21)) has been applied to SWATH CVA for the zero-speed, beam-wave condition. The amplitude and phase of the transverse bending moment TVBM, transverse force TF, and vertical shear force VS acting midpoint of the crossbeam are shown in Figures 2 through 7. The theoretical prediction is indicated by the solid line, and the circles denote experimental values obtained from Reference 2.

TABLE 4 - CHARACTERISTICS OF SMALL-WATERPLANE-AREA, TWIN-HULL MODELS

Characteristic	SWATH CVA	SWATH 1	SWATH 4
Model No.	5266	Modcat 1	5287
Scale Ratio	50	40.96	20.4
Length in Feet:			
Overall	850	520	287.6
Waterline	751	440	226.7
Draft in Feet	69.5	40.0	28.0
Demihull Beam in Feet:			
Waterline	30.42	17.06	8.0
Maximum	70.0	30.72	18.0
Hull Separation in Feet C_L to C_L	279.0	87.5	75.0
Displacement in Long Tons	101000	22600	3960
Waterplane Area in Square Feet	23660	13700	2700
Demihull Projected Side Area in Square Feet	53250	19050	6760
Maximum Sectional Area Demihull in Square Feet	3020	877	332
Neutral Axis Height from Waterline in Feet	68.2	33.0	21.0
Vertical Center of Gravity from Waterline in Feet	+8.5	0.0	+3.2
Transverse $\overline{GM}$ in Feet	92.0	87.55	8.0
Heave Period τ_H in Seconds	19.8	10.0	10.25
Roll Period τ_ϕ in Seconds	25.46	13.09	17.9

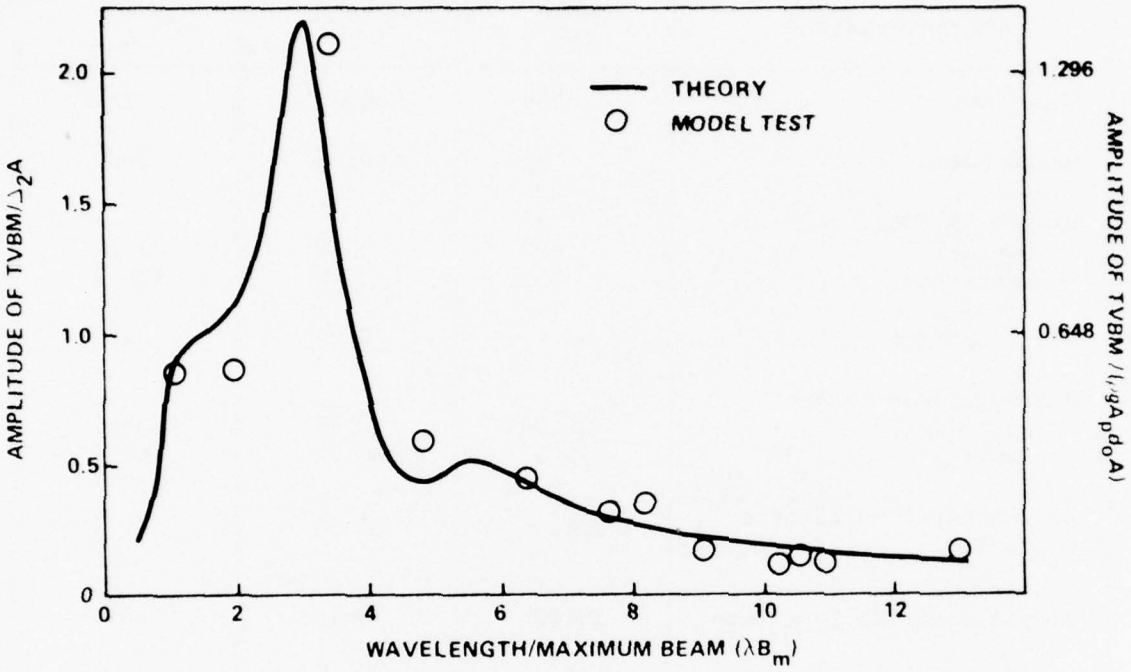

Figure 2 - Amplitude of Transverse Bending Moment of SWATH CVA in Regular Beam Waves

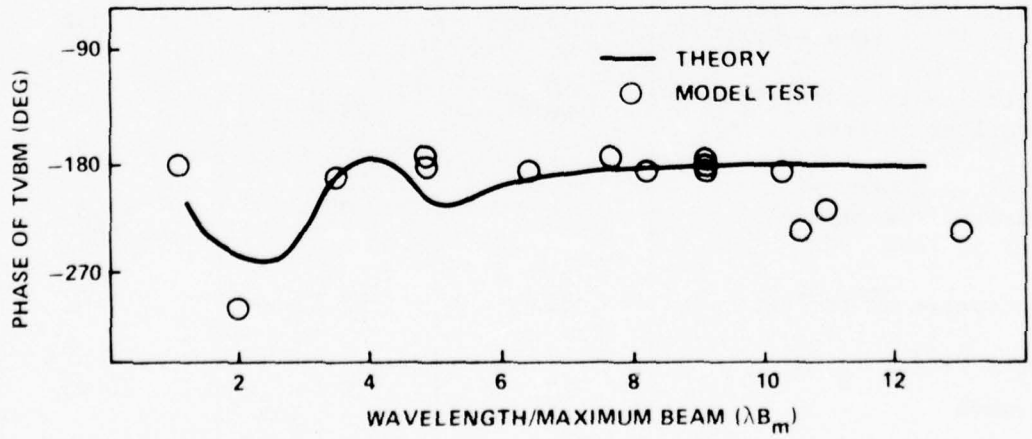

Figure 3 - Phase of Transverse Bending Moment of SWATH CVA in Regular Beam Waves

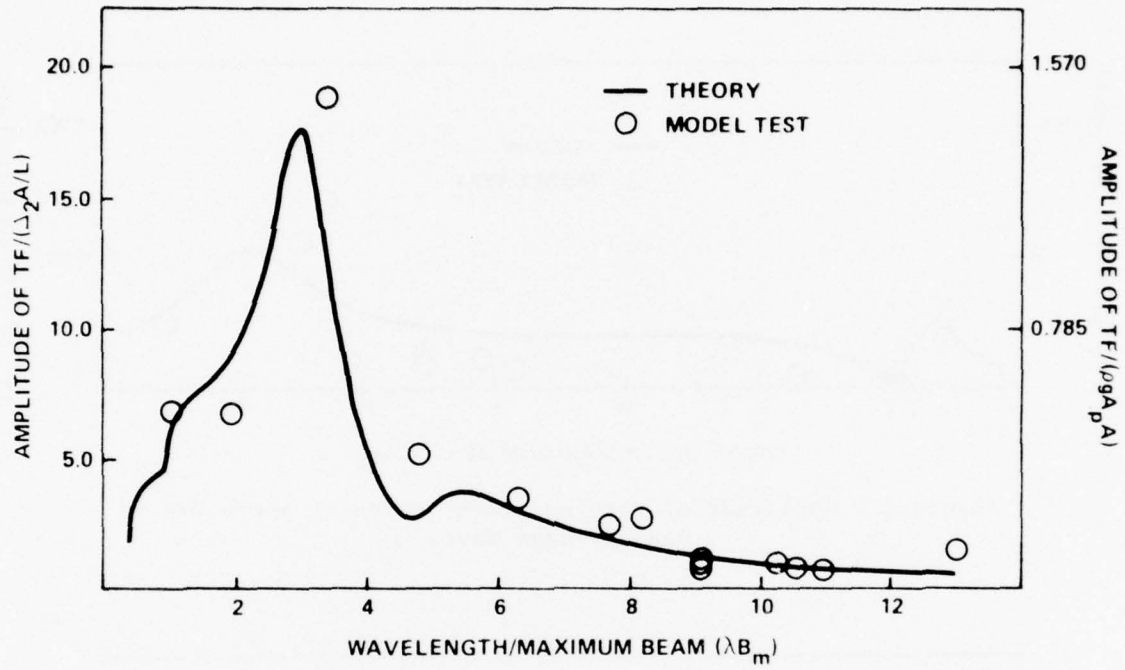

Figure 4 - Amplitude of Transverse Force of SWATH CVA in Regular Beam Waves

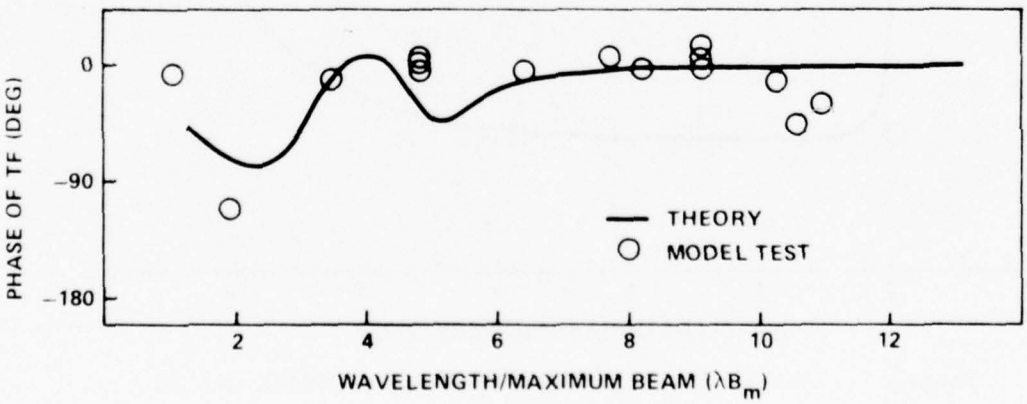

Figure 5 - Phase of Transverse Force of SWATH CVA in Regular Beam Waves

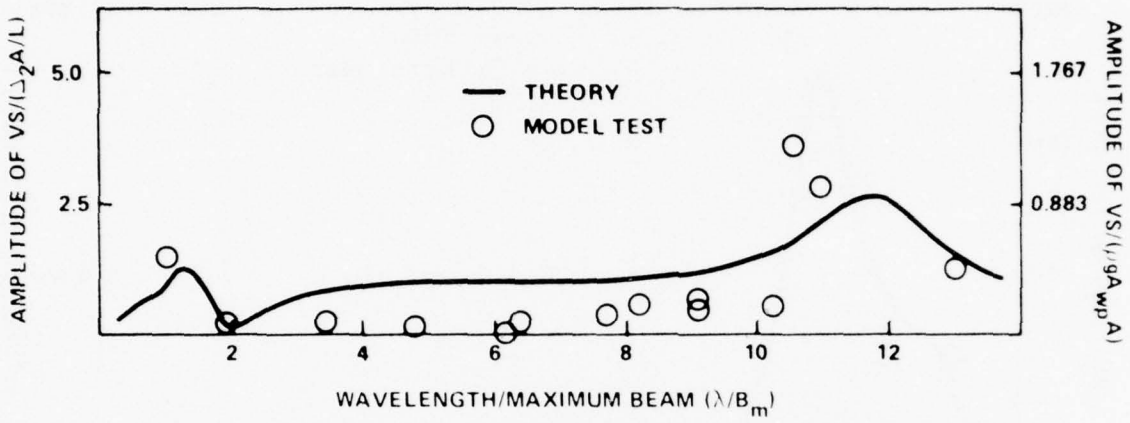

Figure 6 - Amplitude of Vertical Shear Force of SWATH CVA in Regular Beam Waves

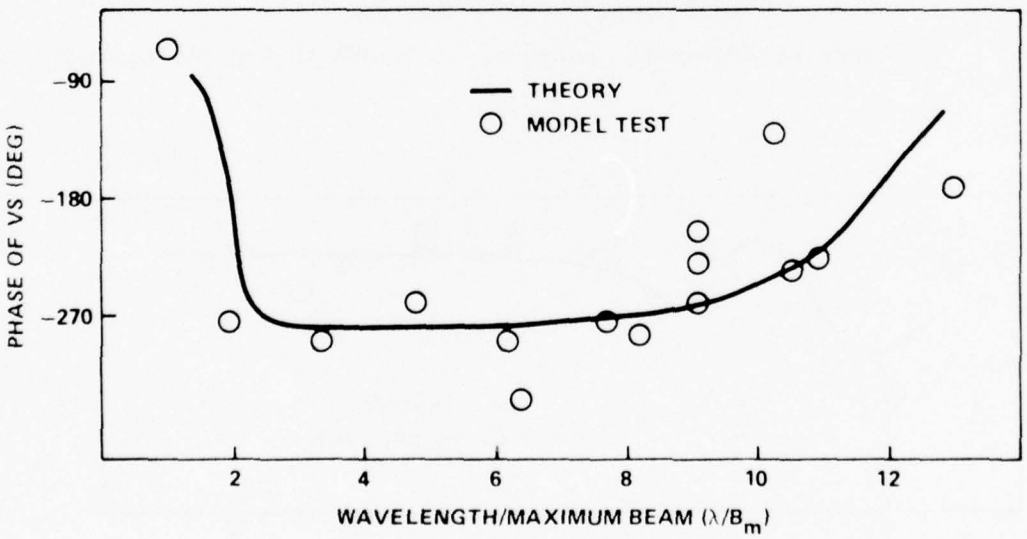

Figure 7 - Phase of Vertical Shear Force of SWATH CVA in Regular Beam Waves

Two scales for the amplitudes of the loads are shown. On the left, vertical scale bending moment is nondimensionalized by the product of ship displacement Δ_2 and wave amplitude A, and the transverse force and vertical shear are nondimensionalized by the product of ship displacement and the ratio of wave amplitude to ship length. On the right, vertical scale bending moment is nondimensionalized by $\rho g A_p dA$, sideload or transverse force by $\rho g A_p A$, and vertical shear by $\rho g A_{wp} A$, where A_p is the side projected area of the submerged portion of the demihull, d is the distance from the netural axis of the cross beam to a point at middraft, and A_{wp} is the waterplane area of the demihull. These nondimensionalizations imply a certain assumed functional dependence of the loads, the significance of which will be described shortly. All phases are specified in degrees relative to the wave crest of the incident-beam wave train at the centerline of the ship.

All of the loads shown in Figures 2 through 7 are at the midpoint of the crossbeam; in linear theory, the maximum bending moment and sideload occur at this point. The loading at other points along the crossbeam and strut will be discussed in a later section.

The heave and roll motions of SWATH CVA are shown in Figures 8 and 9, respectively. Heave motion is nondimensionalized by wave amplitude; the roll motion, by the wave slope $\left(\frac{2\pi A}{\lambda}\right)$.

SWATH 4

An extensive experimental program in which wave loads were measured has also been performed on a 20.4-scale model, DTNSRDC Model 5287, designated as SWATH 4. The results of this program are presented in Reference 10 and have been used for comparison with the theoretical transverse-load predictions.

Figure 10 shows the theoretical and experimental values of the amplitude of transverse bending moment at the center of the crossbeam for SWATH 4. The theoretical values have been obtained by using Equation (21).

---

[10]Kallio, J.A. and J.J. Ricci, "Seaworthiness Characteristics of a Small Waterplane Area Twin Hull (SWATH IV) Part II," DTNSRDC Departmental Report SPD-620-02 (1976).

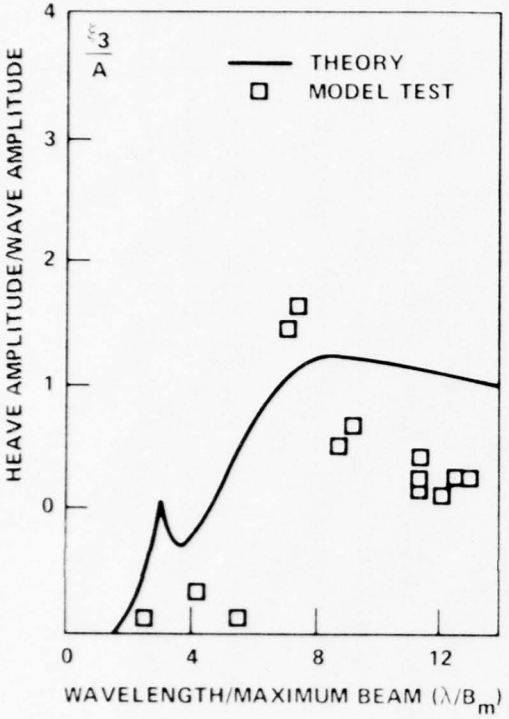

Figure 8 - Amplitude of Heave Motion of SWATH CVA in Regular Beam Waves

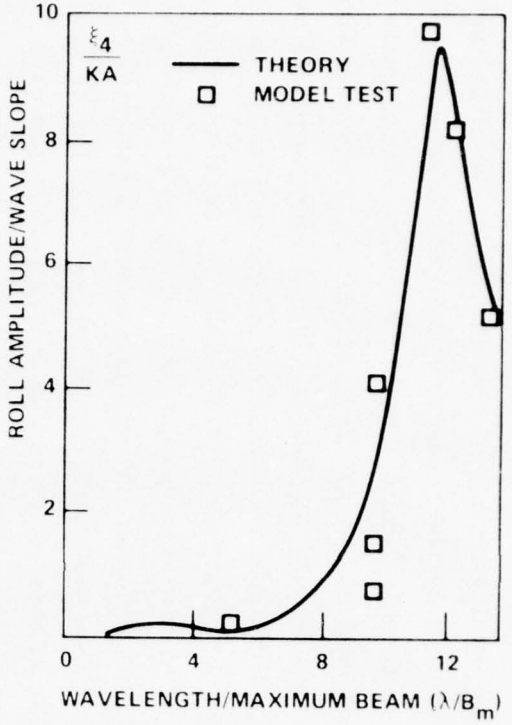

Figure 9 - Amplitude of Roll Motion of SWATH CVA in Regular Beam Waves

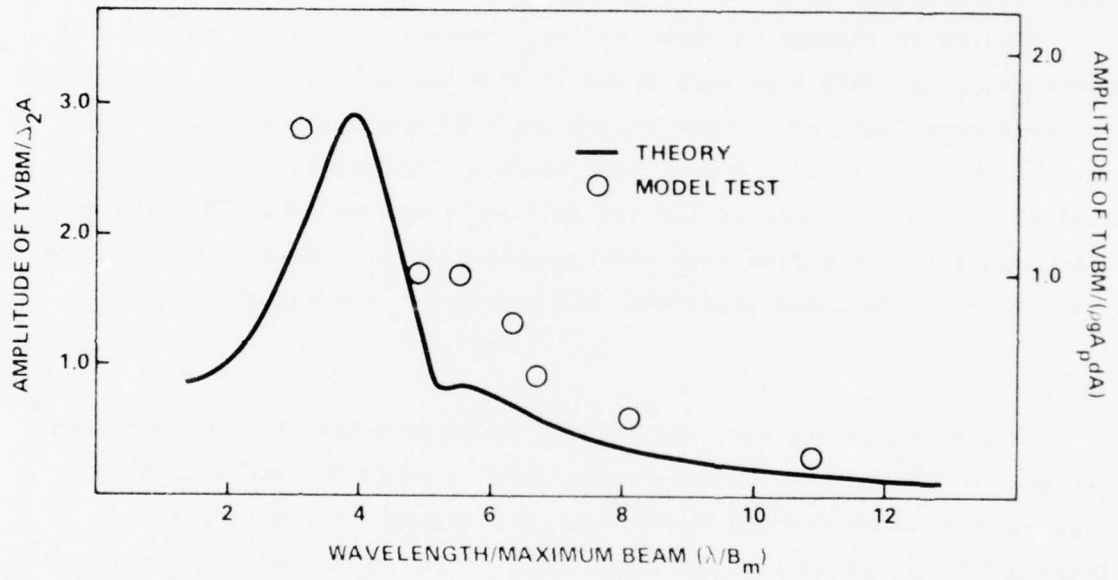

Figure 10 - Amplitude of Transverse Bending Moment of SWATH 4 in Regular Beam Waves

Transverse and vertical shear forces were not measured. However, theoretical values for these quantities obtained by Equations (19) and (20) are presented in Figures 11 and 12. The data have been nondimensionalized in the same manner as those for SWATH CVA. Figure 13 shows the theoretical amplitude of the transverse bending moment obtained by Equation (21) at three points on the ship section for SWATH 4. The solid line denotes response (bending moment) at the centerline of the crossbeam; the dotted line, the response at the juncture of the crossbeam and strut; the broken line, the response on the strut at the waterline.

Figures 14 through 16 show the roll, heave, and sway responses, respectively, of SWATH 4 at zero speed in beam waves. Heave and sway motion are nondimensionalized by wave amplitude; roll angle (radians), by the ratio of wave amplitude to hull separation b. Experimental results are available from Reference 10 for the roll and heave motion. The apparent discontinuity in the predicted sway response (Figure 16) is due to strong coupling from the large predicted roll resonance; see Figure 14.

SWATH 1

Load measurements were obtained on an early model of a SWATH design, designated "SWATH 1." In full-scale, SWATH 1 would be intermediate in size between SWATH CVA and SWATH 4 but with a smaller hull separation. Figures 17 through 19 show the amplitudes of the predicted and experimental transverse bending moment, transverse force, and vertical shear force at the midpoint of the crossbeam. Experimental data for SWATH 1 are unpublished. The data again have been nondimensionalized in the manner described for SWATH CVA.

Load-transfer functions for the three SWATH ships have been used with the Pierson-Moskowitz spectrum, following the approach shown in References 3 and 4, to obtain the statistical loads in irregular beam waves. The significant amplitudes of transverse bending moment, transverse force, and vertical shear force at the midpoint of the crossbeam are shown in Figures 20 through 22 as functions of significant wave height. Bending moment is nondimensionalized by multiplying the demihull displacement Δ_1 by the vertical distance from the neutral axis to middraft d. Transverse force and vertical shear are nondimensionalized by Δ_1.

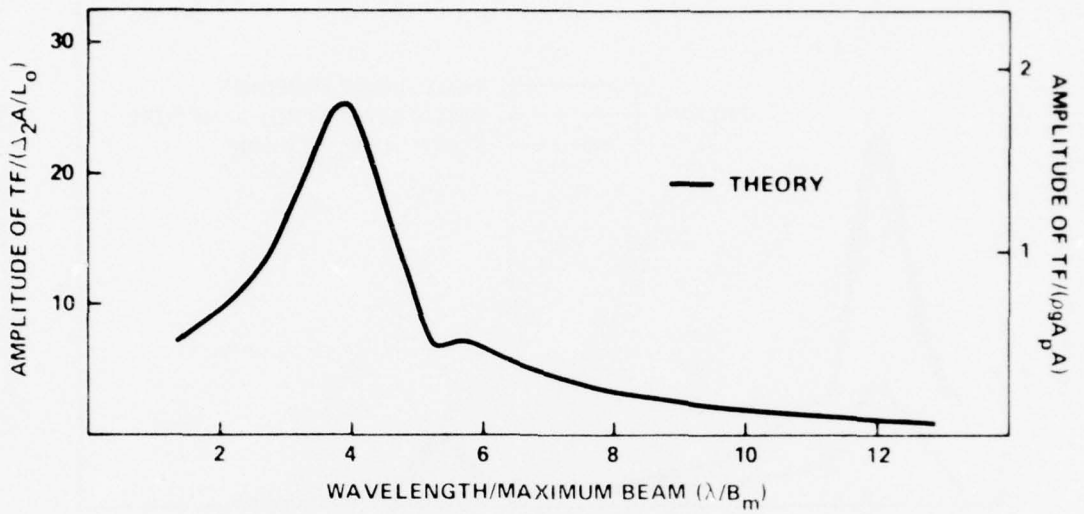

Figure 11 - Amplitude of Transverse Force of SWATH 4 in Regular Beam Waves

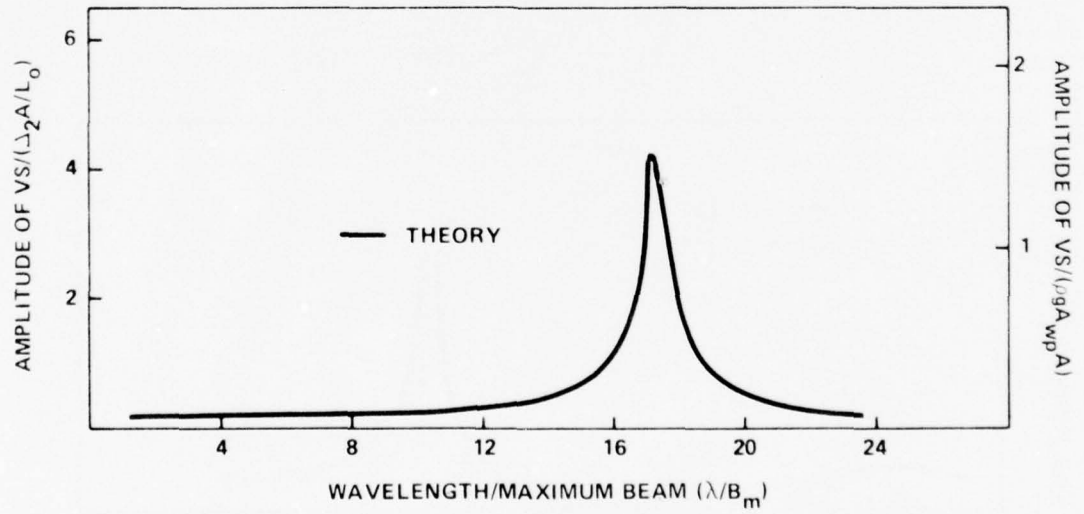

Figure 12 - Amplitude of Vertical Shear Force of SWATH 4 in Regular Beam Waves

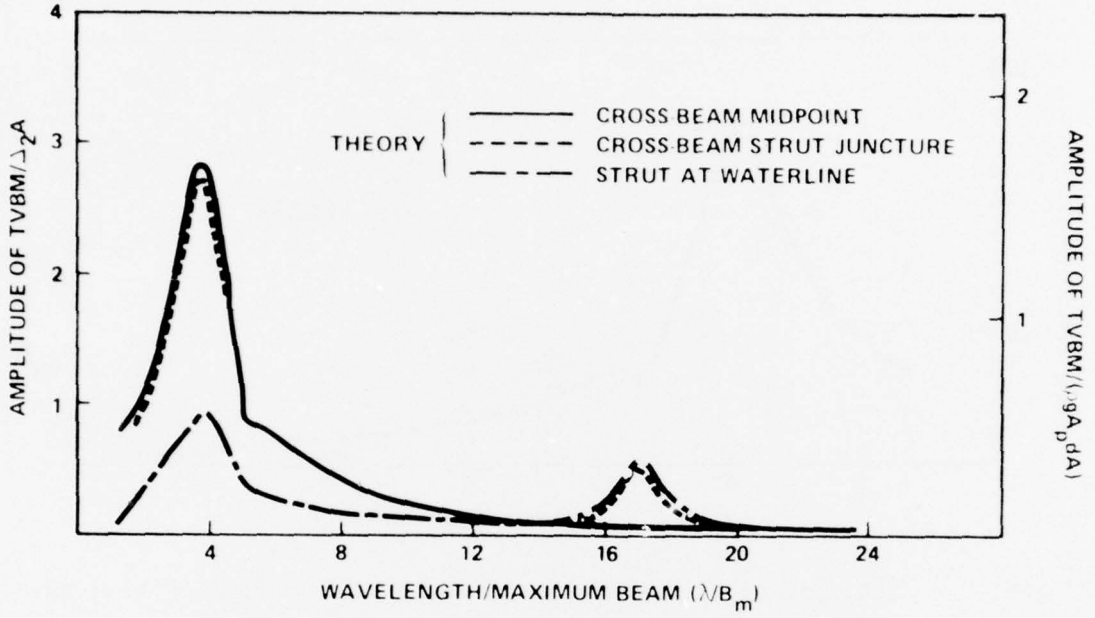

Figure 13 - Amplitude of Transverse Bending Moment of SWATH 4 in Regular Beam Waves at Various Locations on Hull Structure

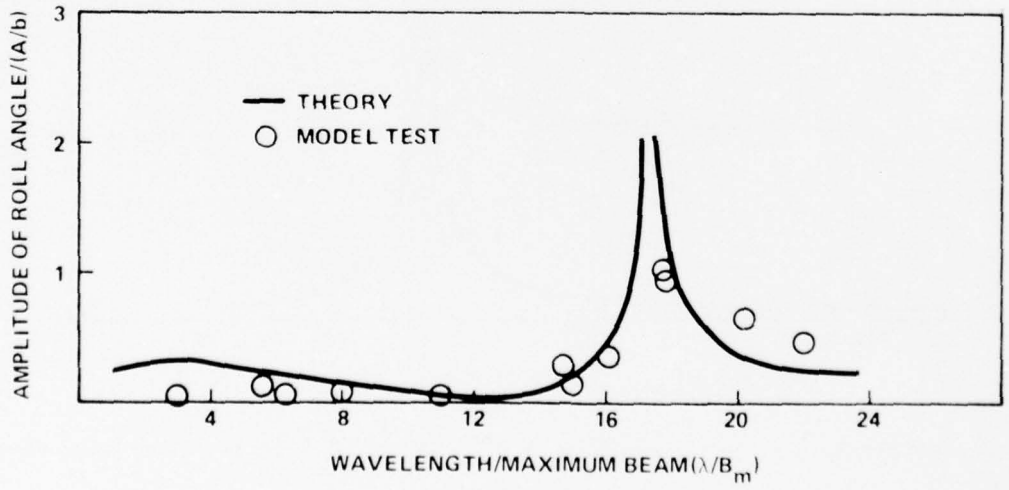

Figure 14 - Amplitude of Roll Motion of SWATH 4 in Regular Beam Waves

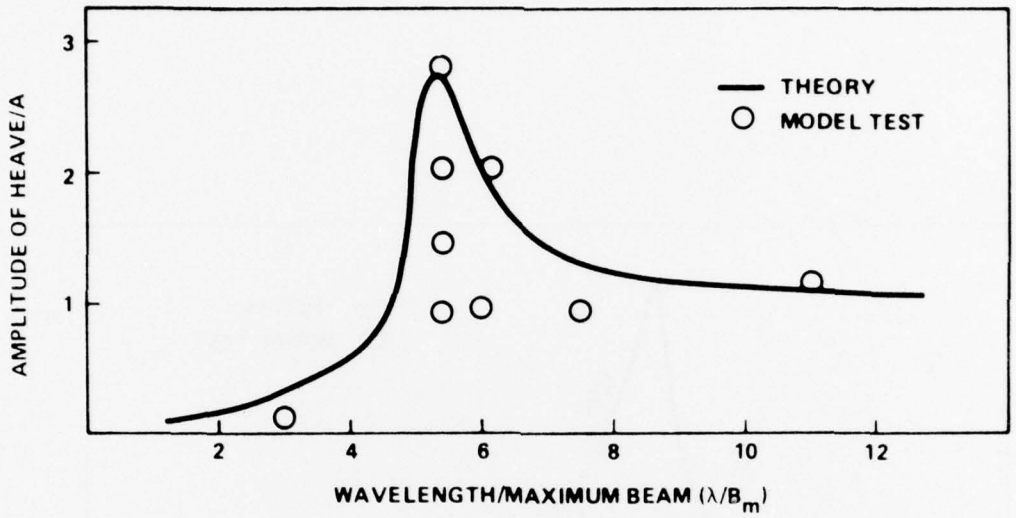

Figure 15 - Amplitude of Heave Motion of SWATH 4 in Regular Beam Waves

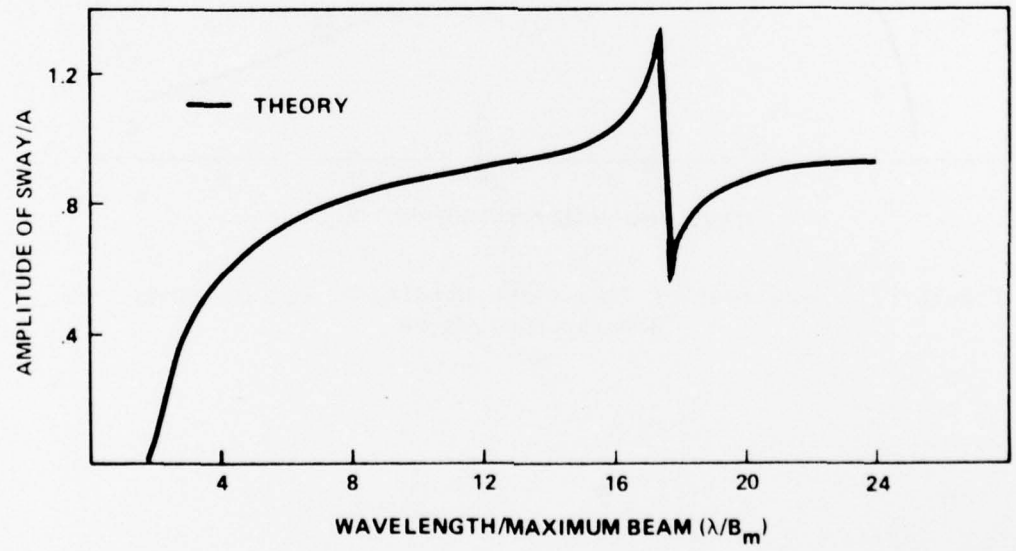

Figure 16 - Amplitude of Sway Motion of SWATH 4 in Regular Beam Waves

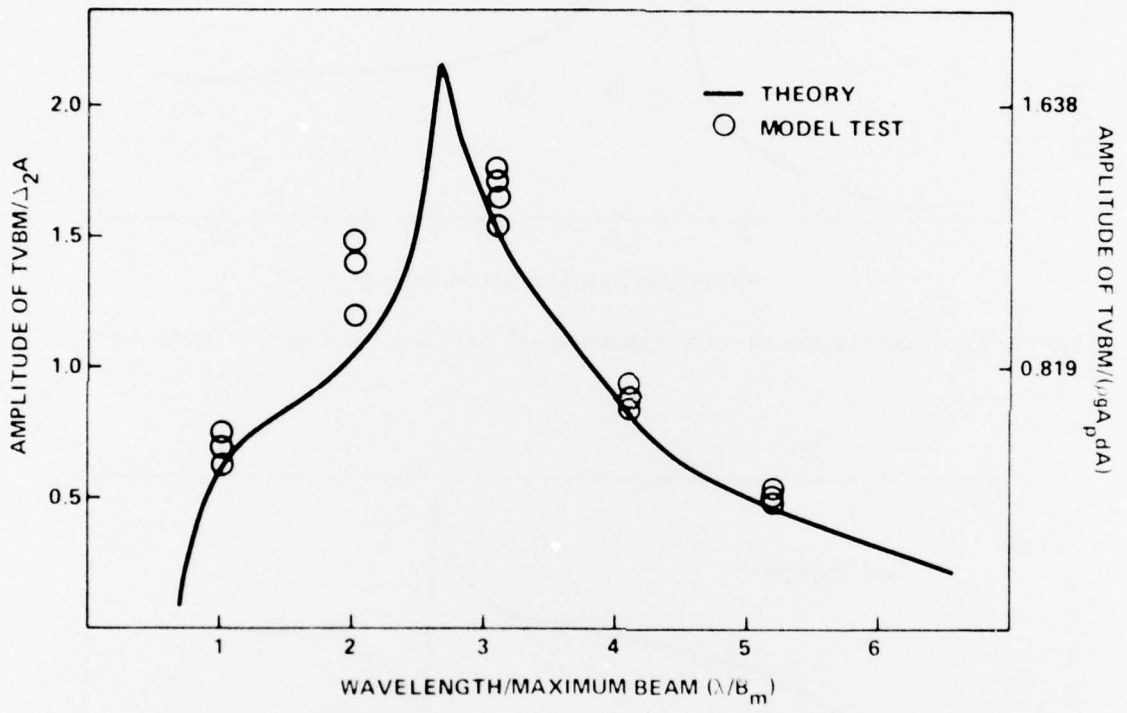

Figure 17 - Amplitude of Transverse Bending Moment of SWATH 1 in Regular Beam Waves

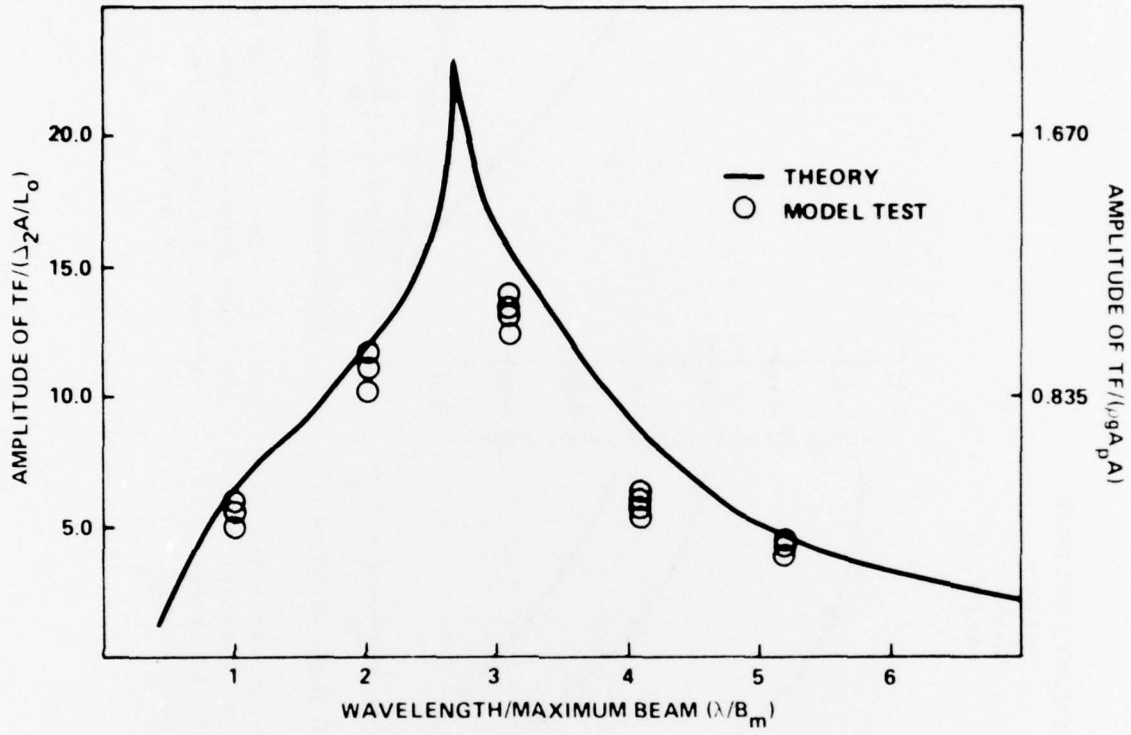

Figure 18 - Amplitude of Transverse Force of SWATH 1 in Regular Beam Waves

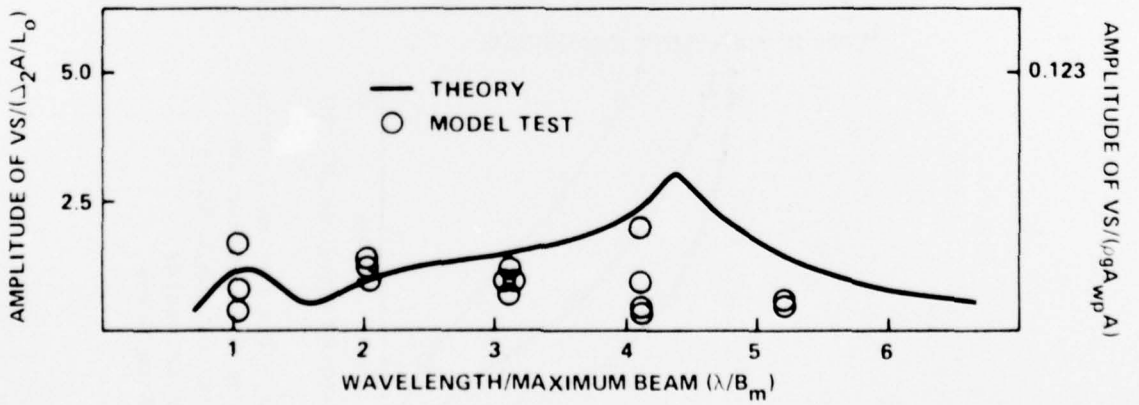

Figure 19 - Amplitude of Vertical Shear Force of SWATH 1 in Regular Beam Waves

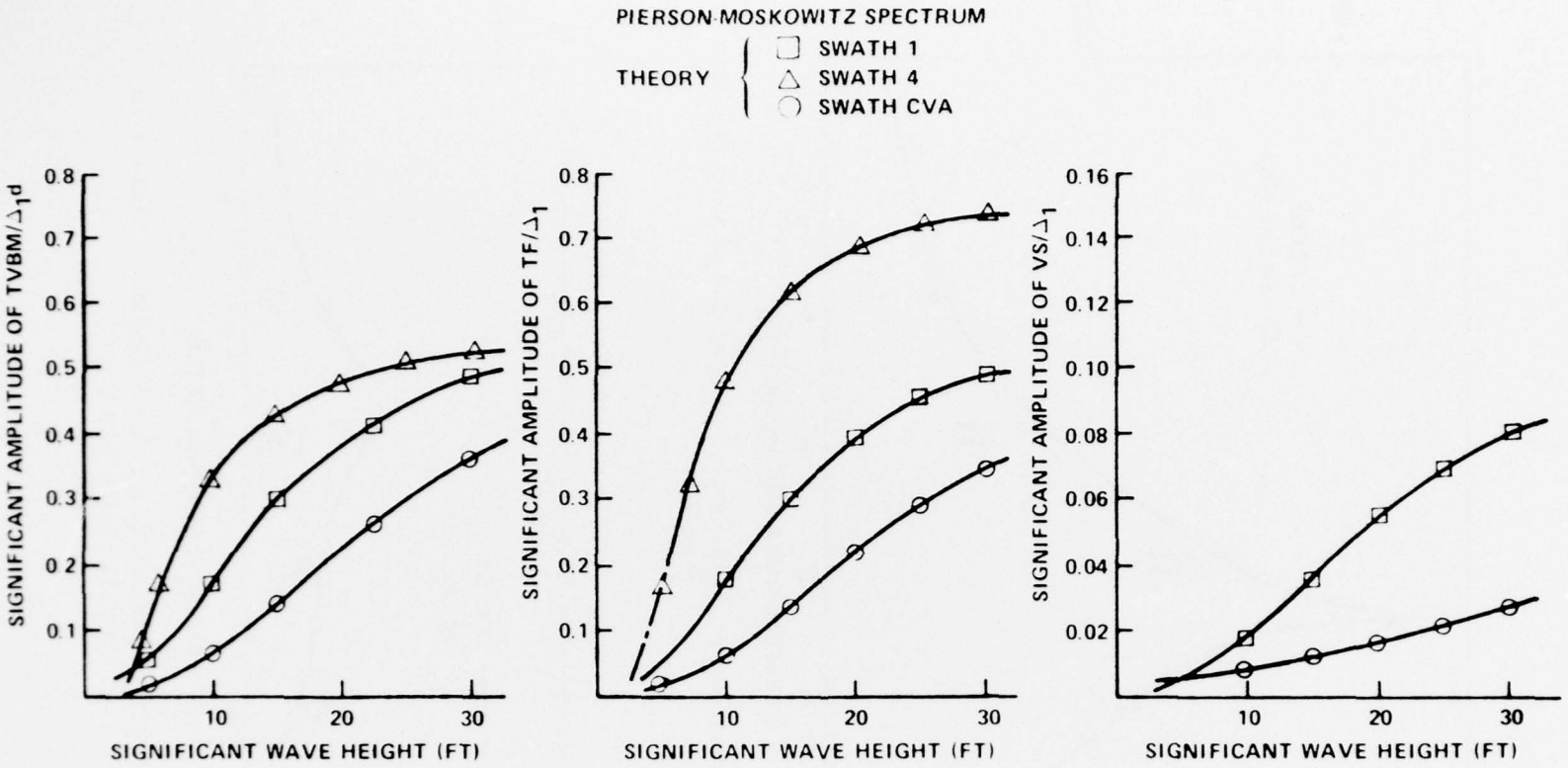

Figure 20 - Transverse Bending Moment at Cross Structure Midpoint of SWATH Hulls in Irregular Beam Waves

Figure 21 - Transverse Force at Cross Structure Midpoint of SWATH Hulls in Irregular Beam Waves

Figure 22 - Vertical Shear Force at Cross Structure Midpoint of SWATH Hulls in Irregular Beam Waves

DISCUSSION OF LOADS ON SMALL-WATERPLANE-AREA, TWIN-HULL SHIPS

The available experimental data generally confirm the validity of the theoretical prediction for the SWATH hull forms. The transverse bending moment and sideload are the more important loads for ship structural requirements and the theory provides very good prediction of these responses. The theory also provides an adequate prediction of the vertical shear on the crossbeam although this load is an order of magnitude smaller than the sideload for SWATH ships.

The essential features of the SWATH loading responses shown in the previous section will now be discussed. Some differences in loading responses among the three SWATH ships are noticeable, and the loads also exhibit some important differences from the loads determined for conventional catamaran hull forms.

In the formulation of the loads, the bending moment, transverse force, and vertical shear force are resolved into components resulting from the effects of the incident wave, diffracted wave, and inertial and hydrodynamic effects of the heave, sway, and roll motion. Furthermore, because of the right-and-left symmetry of the ship section, when loads are evaluated on the axis of symmetry, i.e., the midpoint of the crossbeam, only certain components contribute to any given load quantity. In particular, at the crossbeam midpoint, bending moment arises from the action of horizontal forces which are antisymmetric on the right and left hulls, and vertical forces which are symmetric. The transverse force arises from antisymmetric horizontal forces, and the vertical shear arises from antisymmetric vertical forces; see Equations (19) through (21). Heaving motion produces symmetric vertical inertial and hydrodynamic forces and, therefore, contributes to the bending moment and transverse force. Roll and sway motion produce antisymmetric vertical forces on the hull and contribute to the vertical shear. The wave-exciting and diffraction components contain both symmetric and antisymmetric parts so that the symmetric (even) part contributes to bending moment and transverse force, and the antisymmetric (odd) part contributes to the vertical shear; see Table 3 and Equations (19) through (21).

When loads are computed at points off the ship centerline--along the crossbeam and strut--the problem no longer is symmetric, and all components begin to influence the total load quantities. The theory is formulated, however, so that off-centerline loads can be computed from the centerline loads and additional contributions due to the mass of the crossbeam and strut; see Table 3.

The most prominent feature of the bending moment and transverse-force responses of SWATH ships shown in Figures 2 and 4 is the large peak occurring at wavelengths roughly three to four times the maximum overall beam. This peak is associated with the wave-diffraction contribution, a purely dynamic effect, and would not be predicted by simpler theories based on a "static" approach. Figure 23 shows the midpoint bending moment for SWATH CVA resolved into components arising from incident wave, diffracted wave, and heave motion. The large effect of wave diffraction is apparent. As previously mentioned heave is the only motion contributing to the midpoint bending moment; its effect is small, particularly in the region of peak bending moment. Generally, the wave diffraction is the primary component of the bending moment and transverse force for SWATH ships. By contrast, the incident wave, diffracted wave, and heave motion all provide roughly equal contributions to the bending moment for conventional catamaran hull forms; see Reference 3. Figures 8 and 9 show the heave and roll motion of SWATH CVA; it is noted that the large roll resonance at low frequency has virtually no influence on the midpoint bending moment, as expected. The theory predicts, however, that roll motion should contribute to the vertical shear force, and the small peak in the vertical shear responses for all SWATH ships occurs at the roll resonant frequency. This influence is confirmed by the experimental data; see Figures 6 and 19.

The bending-moment and transverse-force results obtained for SWATH 1 (Figures 17 and 18) are somewhat peculiar in that the responses more closely resemble conventional catamaran hulls than SWATH CVA and SWATH 4. This is probably due to the relatively close hull separation of SWATH 1. The sharp peak at $\lambda/B_m = 3$ in the theoretical results is the result of an exaggerated heave resonance caused by insufficient damping in the motion prediction.

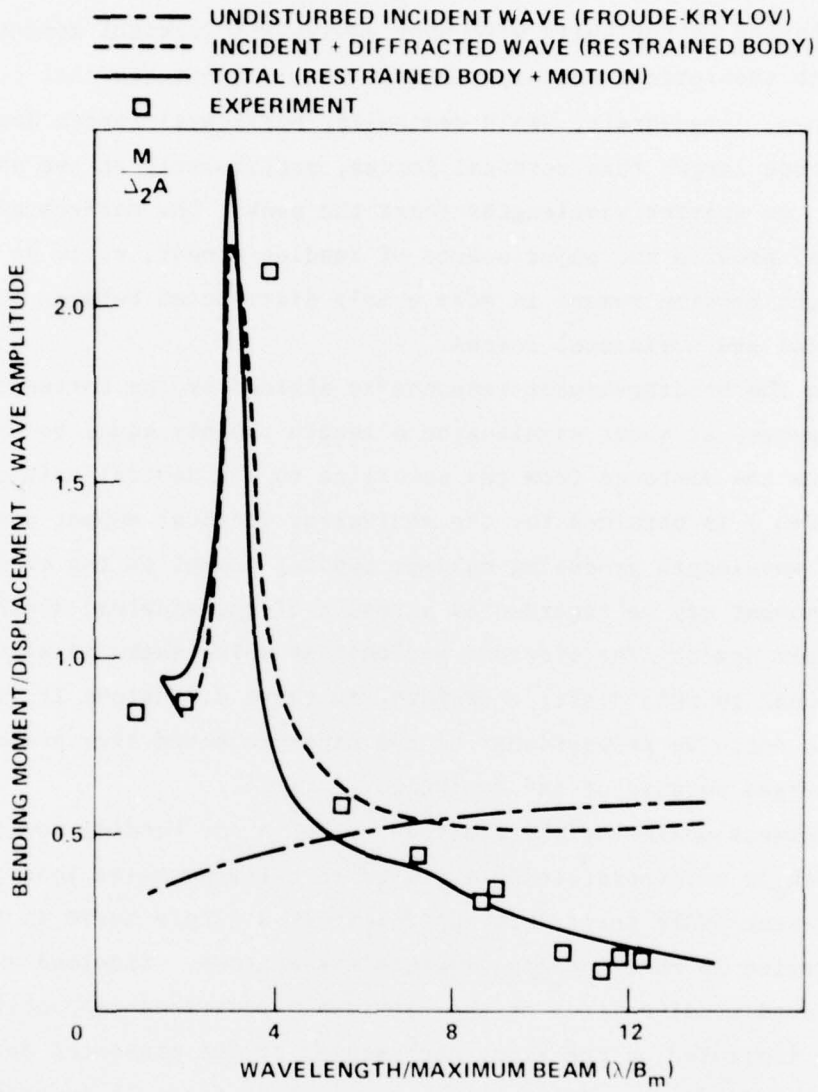

Figure 23 - Decomposition of Bending Moment Effects for SWATH CVA in Regular Beam Waves

It is noted that the bending moment and transverse-force responses for SWATH ships have almost identical shapes. This suggests that the bending moment for SWATH ships is primarily a result of the action of horizontal forces applied on the hulls with some equivalent vertical moment arm. Indeed, both theoretical and experimental results indicate that for the narrow-beam, large-draft, SWATH demihulls, horizontal forces are an order of magnitude larger than vertical forces, particularly at the shorter wavelengths. At shorter wavelengths (near the peak), the horizontal forces (sideload) provide the major source of bending moment, while at longer wavelengths bending moment is more evenly distributed between the action of vertical and horizontal forces.

When the bending-moment response is divided by the corresponding sideload response, at short wavelengths a length roughly equal to the half draft plus the distance from the waterline to the neutral axis of the crossbeam ($H/2+h_o$) is obtained for the equivalent vertical moment arm. Thus, near the wavelength producing maximum bending moment on the crossbeam, the bending moment may be regarded as a result of the sideload acting roughly at the half draft. The sideload per unit of ship length is also roughly proportional to ship draft; therefore, in three dimensions it is expected that this force is proportional to the side-projected area presented by the submerged portion of the demihull.

Nondimensionalizing the sideload by $\rho g A_p A$ and bending moment by $\rho g A_p (H/2+h_o) A$ may therefore be expected to collapse these load quantities for different SWATH ships into approximately a single curve in the wavelength region in which bending moments are maximum. Sideload and bending moment, nondimensionalized by the previously described respective quantities are indicated on the right-hand scales in the presented data.

As previously mentioned the vertical shear force is an order of magnitude smaller than the sideload, except at long wavelengths. The vertical shear is nondimensionalized by $\rho g A_{wp} A$, where A_{wp} is the demihull waterplane area.

In the theoretical formulation, the loads at arbitrary locations along the crossbeam and strut are determined from a knowledge of midpoint loads.

This method is used because midpoint loads exhibit a certain simplicity due to the symmetry of the forces involved. In particular, at the crossbeam midpoint, only heave motion contributes to bending and transverse force, while sway and roll contribute to the vertical shear. This effect is verified by the experimental data shown for SWATH ships.

At points off midpoint of the ship, it is expected that all modes of motion begin to affect the loads. As an example that is typical of SWATH vehicles, the bending-moment response for SWATH 4 is shown in Figure 13 at the crossbeam midpoint, crossbeam strut juncture, and strut at the waterline.

At the midpoint, the peak due to wave diffraction is evident at $\lambda/B_m \sim 4$, and the bending moment decreases to zero in long waves. It is noted that the roll resonance occurring at $\lambda/B_m = 17$ has no effect on the moment at midpoint. (This effect is verified by experimental data as noted in Figure 2 for SWATH CVA.) Moving along the crossbeam to the juncture with the strut, a secondary peak due to roll motion occurs at the roll resonant frequency, with the primary peak almost unaffected. On the strut, the moment is reduced; however, the secondary peak remains unchanged. Although the peak bending moment is greatest at the midpoint, the appearance of the secondary peak at other locations on the crossbeam means that in irregular waves the statistical amplitude of the bending moment could be slightly greater away from midpoint, if the roll resonant frequency were in the vicinity of the peak of the wave spectrum.

CONCLUSIONS

1. A theory for predicting wave-induced transverse bending moment, transverse force (sideload), and vertical shear force on the crossbeam and strut of SWATH ships with zero forward speed in beam waves has been developed. The good agreement between load predictions and available experimental data confirms the basic validity of the theoretical formulation.

2. Due to the large draft and small beam of SWATH demihulls, prediction and model-test results show that horizontally acting loads are an

order of magnitude larger than vertically acting loads. The transverse bending moment acting on the crossbeam is primarily a result of the sideload acting at a point near middraft.

3. The most prominent feature of the sideload and bending-moment responses on the crossbeam is a large peak, due to wave diffraction, occurring at a wavelength roughly three to four times the maximum overall beam of the ship.

4. The peak bending moment in regular waves is maximum at the midpoint of the crossbeam and is in general larger for SWATH ships than for conventional catamarans

$$2 < \frac{\text{Amplitude of peak bending moment}}{\Delta_2 A} < 3$$

where Δ_2 is the displacement of the twin hulls and A is the wave amplitude. However, because of the sharpness of the peak, the bending moment in irregular waves for both SWATH and conventional twin-hull forms is roughly of the same magnitude

$$\frac{\text{Significant amplitude of bending moment}}{\Delta_1 d} < 0.5$$

where Δ_1 is the displacement of one hull, and d is the vertical height from the middraft point to the neutral axis of the crossbeam.

ACKNOWLEDGMENTS

The authors wish to acknowledge the support and encouragement provided by M.D. Ochi during the course of this work.

REFERENCES

1. Curphey, R. M., "Computation of Loads Acting on the Cross Structure and Struts of Twin Hull Ships in Beam Waves," DTNSRDC Departmental Report SPD-651-01 (Nov 1975).

2. Jones, H. D. and D. M. Gerzina, "Motions and Hull-Induced Bridging Structure Loads for a Small Waterplane Area, Twin-Hulled Attack Aircraft Carrier in Waves," NSRDC Report 3819 (Aug 1973).

3. Lee, C. M. et al., "Prediction of Motion and Hydrodynamic Loads of Catamarans," Marine Technology, Vol. 10, No. 4 (Oct 1973).

4. Curphey, R. M. and C. M. Lee, "Analytical Determination of Structural Loading on ASR Catamaran in Beam Seas," NSRDC Report 4267 (Apr 1974).

5. Pien, P. C. and C. M. Lee, "Motion and Resistance of Low-Waterplane Area Catamarans," Ninth Symposium on Naval Hydrodynamics, Vol. 1, Office of Naval Research (1972).

6. Ogilvie, T. F., "On the Computation of Wave-Induced Bending and Torsion Moment," Journal of Ship Research, Vol. 15, No. 3 (1971).

7. Wehausen, J. V. and E. V. Laitone, "Surface Waves," Encyclopedia of Physics, Vol. IX, Spring Verlag (1960).

8. Frank, W., "Oscillation of Cylinders In or Below the Free Surface of Deep Fluids," David Taylor Model Basin Report 2375 (Oct 1967).

9. Lee, C. M. et al., "Added Mass and Damping Coefficients of Heaving Twin Cylinders in a Free Surface," NSRDC Report 3695 (1971).

10. Kallio, J. A. and J. J. Ricci, "Seaworthiness Characteristics of a Small-Waterplane-Area, Twin-Hull (SWATH IV) Part II," DTNSRDC Departmental Report SPD-620-02 (1976).

INITIAL DISTRIBUTION

Copies	
1	CHONR/Code 438, Cooper
2	NRL
	1 Code 2027
	1 Code 2627
3	USNA
	1 NAV SYS TENG DEPT
	1 Prof. Bhattacheryya
	1 Prof. Calisul
2	NAVPGSCOL
	1 Library
	1 Garrison
2	NOSC
	1 Lang
	1 Higdon
1	NCEL/Code 131
3	NAVSEA
	1 SEA 0322/Benen
	1 SEA 03512/Peirce
	1 PMS 300
5	NAVSEC
	1 SEC 6114/Kennell
	1 SEC 6114/Kerr
	1 SEC 6136/Comstock
	1 SEC 6136/Goldstein
	1 SEC 6136/Sandberg
12	DDC
1	NSF/ENGR. Library
1	DOT/Library, TAD-491.1
2	MMA
	1 Capt. McClean
	1 Library
1	NBS/Klebanoff
1	MARAD/Library
1	SNAME/Tech Lib

Copies	
3	U. of CAL/Naval Arch, Berkeley
	1 Webster
	1 Paulling
	1 Wehausen
1	Catholic U. of America/ Civil & Mech Engr
2	U. of HAWAII
	1 St. Denis
	1 Seidl
2	U. of IOWA
	1 IIHR Library
	1 Landweber
1	U. of KANSAS/ Civil Engr Lib
3	MIT
	1 Mandel
	1 Abkowitz
	1 Newman
2	U. of MICH/NAME
	1 Ogilivie
	1 Vorus
2	SOUTHWEST RES INST
	1 Applied Mech Res
	1 Abrahamson
1	Stanford Res Inst/Lib
3	Stevens Inst Tech
	1 Breslin
	1 Savitsky
	1 Kim
1	U. of TEXAS/Arl Lib
2	U. of WASHINGTON
	1 Engr. Library
	1 Mech. Engr./Adee
3	WEBB INST.
	1 Library
	1 Lewis
	1 Ward

Copies	
1	Woods Hole/Ocean Engr.
2	ABS 1 Cheng 1 Library
1	Exxon, NY/Design Div, Tank Dept
1	Gibbs & Cox/Tech Info
2	Hydronautics 1 Library 1 Oceanics
2	Lockheed, Sunnyvale 1 Potash 1 Chung
1	Maritime Res Info Service
1	Newport News Shipbuilding/Lib
1	Robert Taggart
1	Sperry Rand/Tech Lib
1	Sun Shipbuilding/Chief Naval Arch.

Copies	Code	
1	1552	
1	1556	
1	156	
5	1561	
1	1562	
1	1564	
10	1564	Curphey
1	1568	
1	1572	
3	1573	
1	1576	
1	1805	
30	5214.1	Reports Distribution
1	522.1	Unclass Library (C)
1	522.2	Unclass Library (A)

CENTER DISTRIBUTION

Copies	Code	
1	117	Hawkins
1	117	Stevens
1	117	Lamb
1	117	Meyer
1	1502	
1	1506	
2	1507	
1	1509	
1	152	
1	1521	
2	1524	
2	1532	
1	154	
1	1548	

DTNSRDC ISSUES THREE TYPES OF REPORTS

(1) DTNSRDC REPORTS, A FORMAL SERIES PUBLISHING INFORMATION OF PERMANENT TECHNICAL VALUE, DESIGNATED BY A SERIAL REPORT NUMBER.

(2) DEPARTMENTAL REPORTS, A SEMIFORMAL SERIES, RECORDING INFORMATION OF A PRELIMINARY OR TEMPORARY NATURE, OR OF LIMITED INTEREST OR SIGNIFICANCE, CARRYING A DEPARTMENTAL ALPHANUMERIC IDENTIFICATION.

(3) TECHNICAL MEMORANDA, AN INFORMAL SERIES, USUALLY INTERNAL WORKING PAPERS OR DIRECT REPORTS TO SPONSORS, NUMBERED AS TM SERIES REPORTS; NOT FOR GENERAL DISTRIBUTION.